Electronic Supplementary Material (ESI) for Nanoscale.

Supplementary Information for

The rise of MAX phase alloys - large-scale theoretical screening for prediction of chemical order and disorder

Martin Dahlqvist*, Johanna Rosen*

Materials Design, Department of Physics, Chemistry and Biology (IFM), Linköping University, SE-581 83 Linköping, Sweden

* corresponding authors: martin.dahlqvist@liu.se; johanna.rosen@liu.se

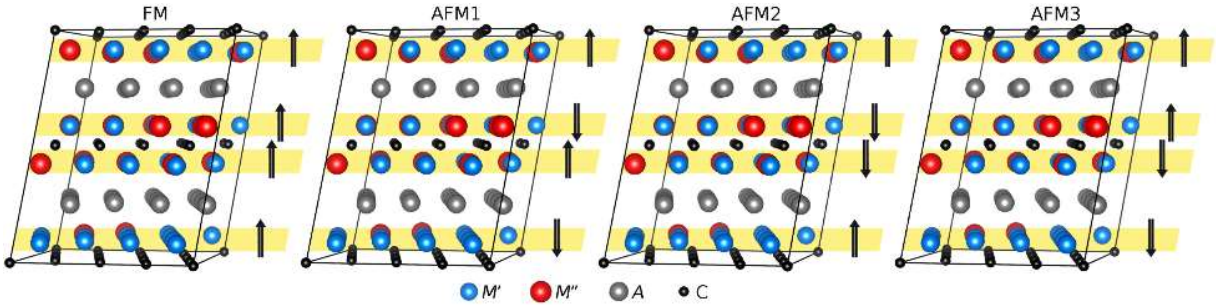

Supplementary Fig. 1. Schematic illustration of considered spin configurations for disordered solid solution MAX phases in a 120 atom supercell.

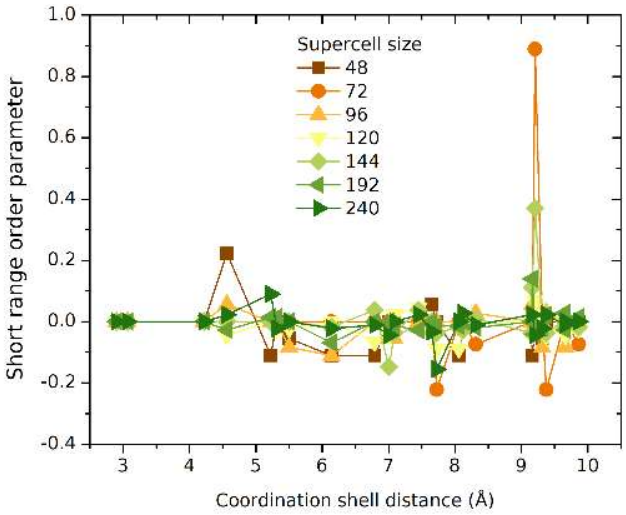

Supplementary Fig. 2. Short rang order parameter of the *M* sublattice as function of coordination shell distance for different supercell sizes considered when generating SQS supercells.

Supplementary Table 1. Experimentally reported quaternary 211 *M*-site solid solution MAX phases.

Year	*Phase*	*Reported x values*	*References*
1980	$(Ti_xV_{1-x})_2AlC$	≤ 0.8	1, 2, 3, 4
1980	$(V_xCr_{1-x})_2AlC$	0 < x < 1	1, 2, 5, 6, 7
1980	$(Ti_xCr_{1-x})_2AlC$	0.02, 0.25, ≥ 0.75	1, 8
1980	$(Ti_xNb_{1-x})_2AlC$	0 < x < 1	1, 4, 9, 10, 11
1982	$(V_xTa_{1-x})_2AlC$	0.65	12
2019	$(Hf_xTa_{1-x})_2AlC$	x < 0.25	13
1983	$(Ti_xTa_{1-x})_2AlC$	0.4	12, 14
2017	$(Ti_xZr_{1-x})_2AlC$	≤ 0.2, ≥ 0.55	15, 16
1980	$(V_xNb_{1-x})_2AlC$	0 < x < 1	4, 12, 17, 18
2013	$(Cr_xMn_{1-x})_2AlC$	≥ 0.8	19, 20, 21
2014	$(Zr_xNb_{1-x})_2AlC$	0 < x < 1	17, 22, 23
2018	$(Sc_xNb_{1-x})_2AlC$	0.33	24
2018	$(Ti_xMo_{1-x})_2AlC$	≥ 0.8	25
2017	$(V_xMn_{1-x})_2AlC$	0.96	26
2017	$(Cr_xFe_{1-x})_2AlC$	≥ 0.98	21
2018	$(Cr_xMn_{1-x})_2GaC$	0.5, ≥ 0.7	20, 27, 28, 29
2015	$(Mo_xMn_{1-x})_2GaC$	0.5	30
2009	$(Ti_xZr_{1-x})_2InC$	0.5	31, 32
2002	$(Ti_xHf_{1-x})_2InC$	0.47, 0.5	31, 33
2011	$(Ti_xV_{1-x})_2GeC$	0.5	34
2016	$(Ti_xCr_{1-x})_2GeC$	≥ 0.75	35
2009	$(V_xCr_{1-x})_2GeC$	0 < x < 1	35, 36, 37
2013	$(Cr_xMn_{1-x})_2GeC$	≥ 0.75	35, 38, 39, 40
2016	$(Cr_xMo_{1-x})_2GeC$	≥ 0.5	35
2018	$(Cr_xMn_{1-x})_2AuC$	0.5	29

Supplementary Table 2. Experimentally reported quaternary *i*-MAX phases with *M*-site in-plane chemical order.

Year	*Phase*	*References*
2017	$(Mo_{2/3}Sc_{1/3})_2AlC$	41
2017	$(Mo_{2/3}Y_{1/3})_2AlC$	42
2017	$(Cr_{2/3}Sc_{1/3})_2AlC$	43
2017	$(Cr_{2/3}Y_{1/3})_2AlC$	43
2018	$(W_{2/3}Sc_{1/3})_2AlC$	44
2018	$(W_{2/3}Y_{1/3})_2AlC$	44
2018	$(Cr_{2/3}Zr_{1/3})_2AlC$	45
2017	$(V_{2/3}Zr_{1/3})_2AlC$	42
2019	$(V_{2/3}Sc_{1/3})_2AlC$	46
2019	$(Mo_{2/3}RE_{1/3})_2AlC$ (RE = Ce, Pr, Nd, Sm, Pd, Tb, Dy, Ho, Er, Tm, Lu)	47
2018	$(Mo_{2/3}Sc_{1/3})_2GaC$	48
2018	$(Mo_{2/3}Y_{1/3})_2GaC$	48
2019	$(Cr_{2/3}Sc_{1/3})_2GaC$	49
2019	$(Mn_{2/3}Sc_{1/3})_2GaC$	49
2019	$(Mo_{2/3}RE_{1/3})_2GaC$ (RE = Gd, Tb, Dy, Ho, Er, Tm, Yb, Lu)	50

Supplementary Table 3. Atomic radius and electronegativity (Pauling scale) considered for *M* and *A*. [51, 52]

M	Atomic radius r_M (Å)	Electronegativity (Pauling scale)	*A*	Atomic radius r_A (Å)	Electronegativity (Pauling scale)
Sc	1.62	1.36	Al	1.43	1.61
Y	1.80	1.22	Ga	1.40	1.81
Ti	1.47	1.54	In	1.58	1.78
Zr	1.60	1.33	Si	1.38	1.90
Hf	1.59	1.30	Ge	1.44	2.01
V	1.35	1.63	Sn	1.63	1.96
Nb	1.46	1.60	Ni	1.25	1.91
Ta	1.46	1.50	Pd	1.37	2.20
Cr	1.29	1.66	Pt	1.38	2.28
Mo	1.39	2.16	Cu	1.28	1.90
W	1.39	2.36	Ag	1.44	1.93
Mn	1.27	1.55	Au	1.44	2.54
Fe	1.26	1.83	Zn	1.36	1.65
Co	1.25	1.88			
Ni	1.25	1.91			

Supplementary Table 4. 92 *i*-MAX phases predicted stable. Synthesized phases in bold.

A	*M´*	*M´´*	$\Delta H_{i\text{-MAX}}$ (meV/atom)	Equilibrium simplex	Status
Al	**Mo**	**Y**	**-100.7**	$YMoC_2$, Mo_3Al, YAl_2, YAl_3C_3	synthesized *i*-MAX
Al	**Cr**	**Sc**	**-90.3**	Cr_2AlC, Sc_3AlC, $Sc_2Al_2C_3$, $ScAl_3$	synthesized *i*-MAX
Al	**Cr**	**Zr**	**-58.5**	ZrC, Cr_2AlC, Cr_2Al, $ZrAl_3$	synthesized *i*-MAX
Al	**V**	**Zr**	**-50.3**	V_2AlC, Zr_4AlC_3, Zr_2Al_3, V_2C	synthesized *i*-MAX
Al	**Mo**	**Sc**	**-38.6**	Mo_2ScAlC_2(o-MAX), $(Sc_{2/3}Mo_{1/3})_2AlC$, Mo_3Al, Mo_3Al_8	synthesized *i*-MAX
Al	**Cr**	**Y**	**-32.2**	Cr_2AlC, YAl_2, $Y_2Cr_2C_3$, Cr_7C_3	synthesized *i*-MAX
Al	**W**	**Sc**	**-26.6**	ScW_2AlC_2 (A), W, $ScAl_3$	synthesized *i*-MAX
Al	**V**	**Sc**	**-26.2**	$ScAl_2$, Sc_3AlC, V_2AlC, $V_{12}Al_3C_8$	synthesized *i*-MAX
Al	**W**	**Y**	**-22.3**	WC, W, YAl_2, YWC_2	synthesized *i*-MAX
Al	Mn	Sc	-95.4	Mn_3AlC, $Sc_2Al_2C_3$, MnAl, Sc_3AlC	
Al	V	Hf	-29.1	V_2AlC, Hf_3AlC_2, $HfAl_2$, V_3Al	
Al	Ti	Zr	-28.0	Ti_2AlC, Zr_3AlC_2, Zr_4Al_3, Zr_2Al_3	
Al	Cr	Hf	-24.7	HfC, Cr_2AlC, Cr_2Al, Cr_5Al_{21}	
Al	Nb	Y	-24.7	YAl_2, $Nb_{12}Al_3C_8$, Y_3AlC, Nb_2C	
Al	Sc	W	-24.6	$(W_{2/3}Sc_{1/3})_2AlC$, Sc_3AlC, $Sc_2Al_2C_3$, $ScAl_3$	
Al	Mn	Y	-24.0	Mn_3AlC, YMn_4Al_8, YAl_2, $Y_10Mn_{13}C_{18}$	
Al	Mn	Zr	-22.8	MnAl, ZrC, Mn_3AlC, C	
Al	Cr	Nb	-20.4	Cr_2AlC, Cr_2Al, $NbAl_3$, $Nb_{12}Al_3C_8$	
Al	Cr	Ta	-14.5	Cr_2AlC, Cr_2Al, Ta_2Al, $Ta_{12}Al_3C_8$	
Al	W	Zr	-10.5	WC, C, ZrC, $ZrAl_3$	
Al	Mo	Zr	-9.3	ZrC, Mo_3Al, C, Mo_3Al_8	
Al	Ti	Y	-2.6	Ti_3AlC_2, YAl_2, Y_3AlC, Y_2Al	
Al	V	Y	-0.7	YAl_2, Y_3Al, $V_{12}Al_3C_8$, V_2C	
Au	Ti	Zr	-10.8	$TiC_{0.75}$, $ZrAu_2$, $ZrC_{0.875}$, Ti_3Au	
Cu	Mn	Sc	-43.0	Cu, $ScCu_2$, Sc_3C_4, $Mn_{23}C$	
Cu	Cr	Sc	-3.5	Cu, $ScCu_2$, Cr_7C_3, Sc_2CrC_3	
Cu	Mo	Sc	-1.1	Mo_2C, $ScCu_2$, Cu, Sc_3C_4	
Ga	**Mn**	**Sc**	**-98.8**	Mn_2GaC, $(Sc_{2/3}Mn_{1/3})_2GaC$	synthesized *i*-MAX
Ga	**Cr**	**Sc**	**-80.5**	Cr_3C_2, $ScGa_2$, $(Sc_{2/3}Cr_{1/3})_2GaC$	synthesized *i*-MAX
Ga	**Mo**	**Sc**	**-49.2**	Mo_2ScGaC_2, $ScGa_3$, Mo_3Ga, $(Sc_{2/3}Mo_{1/3})_2GaC$	synthesized *i*-MAX
Ga	**Mo**	**Y**	**-47.2**	Mo_2C, YGa_2, $(Y_{2/3}Mo_{1/3})_2GaC$, C	synthesized *i*-MAX
Ga	Sc	Mo	-72.2	$(Mo_{2/3}Sc_{1/3})_2GaC$, Sc_2MoGaC_2, Sc_3GaC, $ScGa_2$	
Ga	Cr	Zr	-62.4	ZrC, $ZrGa_3$, Cr_2GaC, Cr_7C_3	
Ga	Sc	W	-53.8	Sc_2WGaC_2, $ScGa_2$, W, $Sc_{11}Ga_{10}$	
Ga	V	Sc	-43.9	$ScGa_2$, V_6C_5, V_2GaC, $Sc_{11}Ga_{10}$	
Ga	Mo	Zr	-35.6	ZrC, Mo_2Ga_2C, Mo_3Ga, $MoGa_4$	
Ga	V	Zr	-31.3	V_2GaC, ZrGa, Zr_3GaC_2	
Ga	Mn	Zr	-30.7	ZrC, Mn_2GaC, Mn_3Ga, $MnGa_4$	
Ga	Y	Mo	-24.7	$(Mo_{2/3}Y_{1/3})_2GaC$, Y_3GaC, YGa_2, Y_4C_5	
Ga	Y	W	-23.5	YWC_2, YGa_2, W, Y_3GaC	
Ga	Cr	Hf	-18.6	HfC, $CrGa_4$, $Cr_{23}C_6$	
Ga	V	Hf	-17.1	V_2GaC, Hf_2GaC	
Ga	Sc	V	-13.2	$(V_{2/3}Sc_{1/3})_2GaC$, Sc_3GaC, $ScGa_2$, Sc_3C_4	
Ga	Zr	Mo	-10.4	ZrC, Mo_3Ga, $ZrGa_3$, Zr_4GaC_3	
Ga	Cr	Nb	-6.5	Cr_2GaC, Nb_2GaC	
Ga	Mn	Y	-4.9	YGa_2, C, $Mn_{23}C_6$, $Y_{10}Mn_{13}C_{18}$	
Ga	Sc	Cr	-4.7	$(Cr_{2/3}Sc_{1/3})_2GaC$, $ScGa_2$, Sc_3GaC, Sc_2CrC_3	
Ga	Ti	Sc	-3.3	Ti_3GaC_2, $ScGa_2$, Sc_3GaC, $Sc_{11}Ga_{10}$	
Ga	Zr	W	-3.1	ZrC, W, $ZrGa_3$	
Ga	Nb	Y	-1.8	YGa_2, Nb_2C, Nb_6C_5, Y_5Ga_3	
Ga	Cr	Ta	-0.5	Cr_2GaC, Ta_2C, $CrGa_4$, $Cr_{23}C_6$	
Ga	Fe	Sc	-0.1	C, Sc_3FeC_4, $ScGa_6Fe_6$, Fe_3Ga	
Ge	Sc	Mo	-45.3	Sc_2MoGeC_2, ScGe, $Sc_2Mo_3Ge_4$, C	
Ge	Sc	W	-25.6	ScGe, Sc_2WGeC_2, WC	
Ge	Sc	V	-11.8	ScGe, C, Sc_3GeC, V_6C_5	
Ge	Cr	Sc	-9.5	$ScCrGe_2$, Cr_3C_2, ScGe, C	
Ge	Sc	Cr	-5.2	ScGe, $ScCrC_2$, Cr_3C_2, C	
In	Sc	W	-9.7	Sc_2WInC_2, W, $ScIn_3$, Sc_3InC	
Ni	Mn	Sc	-12.1	$ScNi_2$, C, Sc_3NiC_4, $Mn_{23}C_6$	
Pd	Sc	Y	-29.6	ScPd, Y_4C_5, Sc_4C_3, Y_2C	
Pd	Ti	Y	-0.4	$TiC_{0.75}$, YPd_3, Y	
Pt	Ti	Zr	-22.2	$TiC_{0.875}$, TiPt, $Zr9Pt_{11}$, Ti_3Pt	
Pt	V	Zr	-0.8	V_2C, V_6C_5, $ZrPt_3$, $Zr9Pt_{11}$	
Si	Sc	W	-44.1	Sc_2WSiC_2, SiC, $Sc_2W_3Si_4$, Sc_5Si_3	
Si	Cr	Sc	-29.9	C, $ScCrC_2$. $Sc_2Cr_4Si_5$, Cr_3Si	
Si	Mn	Sc	-13.4	MnSi, Sc_3C_4, Mn_3Si, C	
Si	Sc	Mo	-4.0	Sc_3C_4, $Sc_2Mo_3Si_4$, C, Sc_5Si_3	
Si	Sc	V	-1.2	$Sc_5Si_3C_{0.5}$, SiC, V_6C_5, C	
Si	V	Sc	-1.2	SiC, V_6C_5, $Sc_2V_3Si_4$, $Sc_5Si_3C_{0.5}$	
Zn	Mn	Sc	-99.8	Sc_3C_4,Sc_3Zn_{17}, $Mn_{23}C_6$, $ScZn_3$	
Zn	Mo	Sc	-58.6	Mo_2C, /$Sc_{2/3}Mo_{1/3})_2ZnC$, C, Sc_3Zn_{17}	
Zn	Cr	Sc	-57.4	$ScZn_3$, Cr_7C_3, Sc_2CrC_3	
Zn	Fe	Sc	-52.9	Fe, C, Sc_3FeC_4, Sc_3Zn_{17}	
Zn	V	Hf	-52.7	V_2ZnC, HfC, Hf_3Zn_3C, V_2C	
Zn	V	Zr	-45.5	V_2C, ZrC, $ZrZn_3$	

Zn	Sc	W	-42.4	$(W_{2/3}Sc_{1/3})_2ZnC$, $ScZn_2$, Sc_4C_3, W
Zn	Sc	Mo	-41.1	$(Mo_{2/3}Y_{1/3})_2ZnC$, YZn, Y_2C, Y_4C_5
Zn	Mo	Y	-38.7	Mo_2C, YZn_3, $(Y_{2/3}Mo_{1/3})_2ZnC$, $YMoC_2$
Zn	Ti	Zr	-31.5	$TiC_{0.75}$, Zr_3Zn_3C, Ti_2C, Ti_3Zn_3C
Zn	Cr	Zr	-31.5	ZrC, $ZrZn_{16}$, $Cr_{23}C_6$, Cr_7C_3
Zn	V	Sc	-30.1	$ScZn_2$, ScZn, V_2C, V_6C_5
Zn	Mn	Zr	-27.5	Zn, ZrC, $Mn_{23}C_6$, $MnZn_3$
Zn	Co	Sc	-26.7	Co, C, Sc_3C_4, Sc_3Zn_{17}
Zn	Ti	Hf	-18.4	$HfC_{0.875}$, Ti_3Zn_3C, Ti_2C, Ti_2Zn
Zn	V	Nb	-13.4	V_2C, $NbZn_3$, Nb_6C_5, V_6C_5
Zn	Y	Mo	-11.8	$(Mo_{2/3}Y_{1/3})_2ZnC$, YZn, Y_2C, Y_4C_5
Zn	Fe	Y	-10.2	Fe, C, YZn_3, Y_3C_4
Zn	Mo	Zr	-8.3	ZrC, Mo, Mo_2C, $MoZn_6$
Zn	W	Sc	-6.3	WC, W, $(Sc_{2/3}W_{1/3})_2ZnC$, $ScZn_3$
Zn	Y	W	-5.5	YZn, YWC_2, W, YZn_3
Zn	Nb	Zr	-3.1	Nb_2C, ZrC, $ZrZn_3$
Zn	Cr	Nb	-0.4	Zn, Nb_6C_5, Cr_7C_3, $Cr_{23}C_6$

Supplementary Table 5. 291 stable MAX phases with solid solution of *M′* and *M′′*. Synthesized phases in bold.

A	*M′*	*M′′*	$\Delta H_{disorder}$ (meV/atom)	$\Delta G_{disorder}$ (meV/atom)	Equilibrium simplex	Status
Ag	Ti	Hf	46.4	-8.4	TiAg, HfC, $TiC_{0.75}$, Ag	
Ag	Ti	Zr	48.5	-6.3	$TiC_{0.75}$, ZrAg, Ag	
Ag	Zr	Ti	54.1	-0.7	ZrAg, $TiC_{0.75}$, $ZrC_{0.875}$, Ag	
Al	**Ta**	**Ti**	-18.3	-73.2	Ta_2C, $TaTi_2AlC_2$ (o-MAX), $TiAl_2$, $TaAl_3$	synthesized
Al	**Ti**	**Ta**	-16.5	-71.4	Ti_2AlC, $TaTi_2AlC_2$ (o-MAX), Ta_2C, $TiAl_2$	synthesized
Al	**Ti**	**Nb**	-9.1	-64.0	$NbTi_2AlC_2$ (D), Ti_2AlC, Nb_2Al, $NbAl_3$	synthesized
Al	**Nb**	**Ti**	-8.5	-63.4	$TiNb_2AlC_2$ (o-MAX), Nb_2Al, $NbTi_2AlC_2$ (D), $NbAl_3$	synthesized
Al	Ti	W	-6.4	-61.3	WTi_2AlC_2 (C), C, Ti_3AlC_2, $TiAl_3$	
Al	**V**	**Ti**	1.8	-53.1	V_2AlC, Ti_2AlC	synthesized
Al	**Ti**	**V**	2.8	-52.1	Ti_2AlC, V_2AlC	synthesized
Al	**Ta**	**Hf**	4.8	-50.0	$HfTa_2AlC_2$ (C), $HfAl_2$, Ta_2C	synthesized
Al	**V**	**Cr**	4.9	-50.0	V_2AlC, Cr_2AlC	synthesized
Al	**Cr**	**V**	8.1	-46.8	Cr_2AlC, V_2AlC	synthesized
Al	**Nb**	**Zr**	11.2	-43.7	Nb_4AlC_3, Zr_5Al_4, Nb_2Al	synthesized
Al	Hf	Ta	11.4	-43.5	Hf_3AlC_2, $HfAl_2$, Ta_2C	
Al	Nb	Ta	12.5	-42.4	Nb_2AlC, Ta_2C, $TaNb_2AlC_2$ (o-MAX), $NbAl_3$	
Al	V	W	14.8	-40.0	W, WAl_5, WC, $V_{12}Al_3C_8$	
Al	**Cr**	**Mn**	15.0	-39.8	Cr_2AlC, Mn_3AlC, MnAl, C	synthesized
Al	**Zr**	**Nb**	16.7	-38.2	$ZrNb_2AlC_2$ (o-MAX), Zr_4AlC_3, $ZrAl_2$, Nb_2Al	synthesized
Al	Mn	Cr	16.8	-38.0	Cr_2AlC, Mn_3AlC, MnAl, C	
Al	Ta	V	19.6	-35.3	Ta_2AlC, V_2AlC	
Al	**Nb**	**Sc**	22.1	-32.8	Sc_3AlC, $NbAl_3$, $Nb_{12}Al_3C_8$, Nb_2AlC	synthesized
Al	**V**	**Ta**	22.8	-32.0	V_2AlC, Ta_2AlC	synthesized
Al	Ta	Nb	25.1	-29.8	Ta_2C, $NbAl_3$, $TaNb_2AlC_2$ (o-MAX), $Ta_{12}Al_3C_8$	
Al	Ti	Hf	25.8	-29.1	Ti_2AlC, H_3AlC_2, TiAl	
Al	Nb	Hf	26.1	-28.7	$Hf_2Nb_2AlC_3$, Nb_2Al, $NbAl_3$	
Al	Ti	Mo	27.9	-26.9	Ti_4AlC_3, Mo_3Al, Mo_3Al_8	
Al	**Cr**	**Ti**	28.4	-26.5	$TiCr_2AlC_2$ (o-MAX), Cr_2Al, $TiAl_3$, TiC	synthesized
Al	Ta	Zr	29.6	-25.2	$ZrAl_2$, ZrC, Ta_2C, $Ta_{12}Al_3C_8$	
Al	Hf	Ti	30.1	-24.7	Hf_3AlC_2, TiAl, Ti_2AlC	
Al	Zr	Ta	30.2	-24.7	Ta_2C, Zr_4AlC_3, $ZrAl_2$, Zr_2Al_3	
Al	**Nb**	**V**	31.2	-23.6	Nb_2AlC, V_2AlC	synthesized
Al	Ta	Sc	33.4	-21.4	$ScTa_2AlC_2$(C), $ScAl_2$, Ta_2C	
Al	Hf	Nb	33.5	-21.3	Hf_4AlC_3, Nb_2Al, $NbAl_3$	
Al	**V**	**Nb**	33.7	-21.2	V_2AlC, Nb_2AlC	synthesized
Al	Cr	Mo	35.6	-19.3	Cr_3C_2, Mo_3Al, Mo_3Al_8, C	
Al	Zr	Hf	36.0	-18.8	$HfZr_2AlC_2$ (o-MAX), Zr_2Al_3, ZrAl	
Al	Mn	Fe	38.7	-16.1	Mn_3AlC, C, Fe_3AlC, Fe_5Al_8	
Al	**Ti**	**Cr**	39.8	-15.0	TiC, Cr_2Al, $TiAl_3$, Ti_4AlC_3	synthesized
Al	Hf	Zr	40.8	-14.0	Hf_4AlC_3, Zr_2Al_3, ZrAl	
Al	Mo	V	41.4	-13.5	C, Mo_3Al, V_6C_5, $MoAl_{12}$	
Al	Mo	Cr	41.5	-13.3	C, Mo_3Al, Cr_2Al, Mo_3Al_8	
Al	**Zr**	**Ti**	44.1	-10.8	Zr_3AlC_2, Ti_2AlC, Zr_4Al_3, Zr_2Al_3	synthesized
Al	V	Mo	45.5	-9.4	Mo_3Al, V_6C_5, Mo_3Al_8, $V_{12}Al_3C_8$	
Al	Mn	Mo	47.7	-7.2	C, Mn_3AlC, Mo_3Al, Mo_3Al_8	
Al	Mn	V	47.9	-7.0	MnAl, C, $V_{12}Al_3C_8$, V_6C_5	
Al	Cr	Fe	49.4	-5.5	Cr_2AlC, Fe_3AlC, C, Fe_5Al_8	
Al	W	Ti	50.2	-4.6	C, $Ti_2W_2AlC_3$ (o-MAX), WAl_5	
Al	Mo	Mn	50.9	-4.0	C, Mo_3Al, Mn_3AlC, Mo_3Al_8	
Al	Cr	W	52.8	-2.0	Cr_2AlC, WC, W, WAl_5	
Al	Mo	Nb	54.6	-0.3	C, Mo_3Al, Nb_6C_5, Mo_3Al_8	
Au	Nb	Ta	1.1	-53.8	$NbAu_2$, Ta_2C, Nb_6C_5, Nb_2C	
Au	Ta	Nb	3.7	-51.1	Ta_2C, Au, $NbAu_2$, Nb_6C_5	
Au	V	Ta	17.8	-37.1	V_2AuC, Ta_2C, Au	
Au	Ta	V	18.8	-36.0	Ta_2C, Au, V_2AuC	
Au	Nb	V	23.8	-31.1	Nb_2AuC, V_2AuC	
Au	Ti	Nb	24.6	-30.2	TiA_2, Ti_3AuC_2, Nb_2C	
Au	V	Nb	24.7	-30.1	V_2AuC, Nb_2AuC	
Au	Ti	Ta	27.9	-27.0	$TiAu_2$, Ti_2AuC_2, Ta_2C	
Au	Nb	Ti	28.6	-26.3	$TiAu_2$, Nb_2C, Nb_6C_5, Ti_3AuC_2	
Au	Ti	V	31.2	-23.6	$TiAu_2$, Ti_3AuC_2, V_2C	
Au	Zr	Hf	32.4	-22.4	HfC, $ZrC_{0.875}$, $ZrAu_2$, Zr_2Au	
Au	Ta	Ti	33.1	-21.7	$TiAu_2$, Ta_2C, Ta_4C_3, $Ti_3Au_2C_2$	
Au	V	Ti	34.6	-20.2	$TiAu_2$, V_2C, $Ti_3Au_2C_2$, V_6C_5	
Au	Ti	Hf	38.1	-16.7	HfC, Ti_3AuC_2, $HfAu_2$, Ti_3Au	
Au	Zr	Ti	38.9	-15.9	$ZrC_{0.875}$, $ZrAu_2$, $TiC_{0.75}$, Ti_3Au	
Au	Hf	Zr	41.6	-13.2	HfC, HfAu, $ZrAu_2$, Zr_2Au	
Au	Hf	Ti	46.3	-8.6	HfC, $HfAu_2$, Ti_3Au, Ti_3AuC_2	
Au	V	Cr	49.7	-5.2	Au, Cr, V_2C, V_6C_5	
Au	V	Mo	51.3	-3.5	Au, Mo, V_2C, V_6C_5	
Au	Hf	Nb	51.9	-2.9	HfC, $HfAu_2$, HfAu, Nb_2C	
Au	Ti	Mo	52.0	-2.9	$Ti_3Au_2C_2$, Mo, Mo_2C, $TiAu_4$	
Au	Ta	Mo	52.5	-2.3	Au, Mo, Ta_4C_3	
Au	Zr	Nb	52.7	-2.2	$ZrC_{0.875}$, $ZrAu_2$, Nb_2C, Zr_2Au	

Au	Nb	Mo	53.1	-1.7	Au, Mo, Nb_6C_5, $NbAu_2$	
Ga	Ta	Ti	-36.9	-91.8	Ta_2GaC, Ti_2GaC	
Ga	Ti	Ta	-35.3	-90.2	Ti_2GaC, Ta_2GaC	
Ga	Ti	W	-24.7	-79.5	W, Ti_3GaC_2, WC, $TiGa_3$	
Ga	Ti	Nb	-19.1	-73.9	Ti_2GaC, Nb_2GaC	
Ga	Nb	Ti	-18.9	-73.7	Nb_2GaC, Ti_2GaC	
Ga	Sc	Ta	-14.3	-69.2	TaC, $ScGa_2$, Sc_3GaC	
Ga	Ta	Hf	-13.6	-68.4	Ta_2GaC, HfG_2, Hf_3GaC_2, Ta_2C	
Ga	Nb	Sc	-13.0	-67.9	$(Sc_{2/3}Nb_{1/3})_2GaC$, Nb_2GaC	
Ga	Hf	Ta	-10.9	-65.8	$HfGa_2$, Hf_3GaC_2, Ta_2C	
Ga	Ti	Mo	-8.0	-62.9	Ti_3GaC_2, Ti_2MoGaC_2 (o-MAX), Mo_3Ga, $MoGa_4$	
Ga	Sc	Nb	-7.7	-62.6	$(Nb_{2/3}Sc_{1/3})_2GaC$, Sc_3GaC, $ScGa_2$, Sc_3C_4	
Ga	Nb	Zr	-2.9	-57.8	Nb_2GaC, ZrGa, Zr_3GaC_2	
Ga	Ti	V	-2.6	-57.5	Ti_2GaC, V_2GaC	
Ga	V	Ti	-2.0	-56.8	V_2GaC, Ti_2GaC	
Ga	Ta	Nb	-2.0	-56.8	Ta_2GaC, Nb_2GaC	
Ga	Nb	Ta	-1.9	-56.8	Nb_2GaC, Ta_2GaC	
Ga	Nb	Hf	-1.8	-56.7	Nb_2GaC, Hf_3GaC_2, Nb_5Ga_4, Nb_5Ga_{13}	
Ga	Zr	Nb	1.6	-53.3	Nb_2GaC, ZrGa, Zr_3GaC_2	
Ga	Ta	Sc	6.2	-48.7	$ScGa_2$, $(Sc_{2/3}Ta_{1/3})_2GaC$, Ta_2C, Ta_4C_3	
Ga	Hf	Nb	6.4	-48.4	Hf_3GaC_2, Nb_2GaC, Nb_5Ga_4, Nb_5Ga_{13}	
Ga	V	Cr	6.5	-48.3	V_2GaC, Cr_2GaC	
Ga	Cr	V	8.2	-46.7	Cr_2GaC, V_2GaC	
Ga	V	Mo	8.9	-46.0	V_6C_5, V_2GaC, MoG_4, Mo_3Ga	
Ga	Ta	Zr	10.7	-44.2	Ta_4C_3, Zr_3Ga_5, Ta_2C, Zr_3GaC_2	
Ga	Zr	Ta	10.7	-44.2	Zr_3GaC_2, Ta_2C, Zr_3Ga_5, Ta_4C_3	
Ga	**Mn**	**Cr**	11.9	-43.0	Mn_2GaC, Cr_2GaC	synthesized
Ga	Cr	Ti	14.2	-40.7	Cr_2GaC, Ti_3GaC_2, $CrGa_4$, $Cr_{23}C_6$	
Ga	Mo	V	14.2	-40.7	Mo_2Ga_2C, Mo_3Ga, V_6C_5, Mo_2C	
Ga	**Cr**	**Mn**	14.8	-40.0	Cr_2GaC, Mn_2GaC	synthesized
Ga	Ta	V	16.7	-38.2	Ta_2GaC, V_2GaC	
Ga	Hf	Ti	18.8	-36.0	Hf_2GaC, Ti_2GaC	
Ga	V	Ta	18.9	-36.0	V_2GaC, Ta_2GaC	
Ga	Ti	Hf	19.0	-35.8	Ti_2GaC, Hf_2GaC	
Ga	Ti	Cr	19.1	-35.7	Ti_3GaC_2, $CrGa_4$, Cr, $Cr_{23}C_6$	
Ga	Mo	Nb	22.8	-32.0	Mo_2Ga_2C, Nb_4GaC_3, Mo_2C, Mo_3Ga	
Ga	Cr	Mo	24.8	-30.1	Cr_2GaC, Mo_2Ga_2C, Mo_2C	
Ga	Nb	Mo	25.2	-29.7	Nb_4GaC_3, Mo_3Ga, $MoGa_4$	
Ga	Mo	Cr	26.5	-28.4	Mo_2Ga_2C, Cr_2GaC, Mo_2C	
Ga	Mn	V	26.6	-28.2	Mn_2GaC, V_2GaC	
Ga	V	W	26.8	-28.0	V_2GaC, WC, W	
Ga	V	Mn	27.0	-27.9	V_2GaC, Mn_2GaC	
Ga	Nb	V	28.5	-26.3	Nb_2GaC, V_2GaC	
Ga	V	Nb	30.6	-24.3	V_2GaC, Nb_2GaC	
Ga	Mo	Ti	31.6	-23.2	Mo_2TiGaC_2 (o-MAX), $(Ti_{2/3}Mo_{1/3})_2GaC$, Mo_3Ga, $MoGa_4$	
Ga	Zr	Hf	32.6	-22.2	ZrGa, HfC, Zr_3GaC_2	
Ga	**Mn**	**Mo**	32.9	-21.9	Mn_2GaC, Mo_2Ga_2C, Mo_2C	synthesized
Ga	Mn	Fe	34.2	-20.6	Mn_2GaC, C, Fe_3Ga, $FeGa_3$	
Ga	**Mo**	**Mn**	34.3	-20.6	Mn_2GaC, Mo_2Ga_2C, Mo_2C	synthesized
Ga	Ti	Zr	36.8	-18.0	ZrGa, Ti_3GaC_2, Zr_3GaC_2	
Ga	Hf	Zr	40.7	-14.1	ZrGa, Hf_4GaC_3	
Ga	Zr	Ti	42.1	-12.8	ZrGa, Zr_3GaC_2, Ti_3GaC_2	
Ga	Ta	Mo	45.6	-9.2	Ta_4C_3, Mo_3Ga, $MoGa_4$	
Ga	Mo	Ta	46.7	-8.1	TaC, Mo_2Ga_2C, Mo_3Ga, $MoGa_4$	
Ga	Nb	W	49.4	-5.5	Nb_2GaC, WC, W, Nb_5Ga_{13}	
Ga	Ta	W	49.7	-5.1	Ta_2GaC, WC, W, Ga	
Ga	Hf	V	53.8	-1.0	Hf_2GaC, V_2GaC	
Ge	Sc	Nb	-21.3	-76.2	ScGe, C, Nb_6C_5, Sc_3GeC	
Ge	Ti	Ta	-18.9	-73.8	Ti_2GeC, Ta_2GeC	
Ge	Ta	Ti	-12.5	-67.3	Ta_2GeC, Ti_2GeC	
Ge	Sc	Ta	-9.4	-64.2	ScGe, TaC, Sc_3GeC, C	
Ge	Hf	Ta	-1.6	-56.5	Hf_2GeC, Ta_2GeC	
Ge	Ti	Nb	0.0	-54.8	Ti_2GeC, $NbGe_2$, Nb_5Ge_3C	
Ge	Ta	Hf	2.4	-52.4	Ta_2GeC, Hf_2GeC	
Ge	Nb	Sc	2.5	-52.4	$(Sc_{2/3}Nb_{1/3})_2GeC$, Nb_4GeC_3	
Ge	Nb	Ti	2.5	-52.4	Nb_2GeC, Ti_3GeC_2, $NbGe_2$, Nb_5Ge_3C	
Ge	**V**	**Ti**	5.8	-49.1	V_2GeC, Ti_2GeC	synthesized
Ge	**Ti**	**V**	6.2	-48.6	Ti_2GeC, V_2GeC	synthesized
Ge	Zr	Nb	8.9	-45.9	ZrGe, ZrC, $ZrGe_2$, Nb_6C_5	
Ge	Ti	Mo	10.2	-44.6	Ti_3GeC_2, $MoGe_2$, Mo_2C, Mo_3Ge	
Ge	Nb	Zr	10.3	-44.5	ZrGe, $ZrGe_2$, Nb_6C_5, Nb_2GeC	
Ge	Nb	Ta	11.4	-43.5	TaC, Nb_2GeC, $NbGe_2$, Nb_5Ge_3C	
Ge	**Cr**	**V**	11.6	-43.3	Cr_2GeC, Ge, Cr_3Ge, V_6C_5	synthesized
Ge	**V**	**Cr**	11.9	-43.0	Ge, Cr_3Ge, V_2GeC, V_6C_5	synthesized
Ge	Ta	Sc	14.3	-40.5	ScGe, Ge, Ta_4C_3	
Ge	Ti	W	15.9	-38.9	Ti_2GeC, WC, W, Ge	
Ge	Ta	V	16.3	-38.6	Ta_2GeC, V_2GeC	
Ge	V	Ta	17.5	-37.4	V_2GeC, Ta_2GeC	
Ge	Mo	Ti	18.0	-36.9	Mo_2C, $MoGe_2$, Ti_3GeC_2, C	
Ge	Ta	Nb	18.4	-36.5	$NbGe_2$, Ta_4C_3, Ta_2GeC, $Nb_5Ge_3C_5$	

Ge	Hf	Ti	19.6	-35.3	Hf_2GeC, Ti_2GeC	
Ge	Ti	Hf	19.8	-35.1	Ti_2GeC, Hf_2GeC	
Ge	Cr	Ti	24.3	-30.5	Cr_2GeC, Ti_3GeC_2, Ge, Cr_3Ge	
Ge	Sc	Zr	24.3	-30.5	ScGe, ZrC, Sc_3GeC, C	
Ge	Zr	Sc	24.6	-30.3	ZrC, ScGe, ZrGe	
Ge	Nb	V	28.4	-26.4	Nb_2GeC, V_2GeC	
Ge	V	Nb	29.3	-25.5	V_2GeC, Nb_2GeC	
Ge	Nb	Hf	29.5	-25.3	HfC, $NbGe_2$, Nb_5Ge_3C, Nb_2GeC	
Ge	Zr	Ta	30.1	-24.8	ZrGe, TaC, ZrC	
Ge	**Cr**	**Mn**	30.7	-24.1	MnGe, Cr_3C_2, Ge, C	synthesized
Ge	Zr	Mo	31.5	-23.3	ZrC, $ZrGe_2$, Mo_3Ge, $MoGe_2$	
Ge	Nb	Mo	31.9	-23.0	$MoGe_2$, Nb_6C_5, Nb_2GeC, Mo_3Ge	
Ge	Sc	Ti	32.0	-22.8	ScGe, TiC, Sc_3GeC, C	
Ge	**Ti**	**Cr**	34.5	-20.4	Ti_3GeC_2, Ge, Cr_3Ge, Cr_2GeC	synthesized
Ge	Hf	Nb	35.3	-19.6	HfC, $NbGe_2$, $Hf_2Nb_3Ge_4$	
Ge	Zr	Ti	39.9	-15.0	ZrGe, ZrC, Ti_3GeC_2	
Ge	Hf	Zr	40.6	-14.2	HfC, ZrGe, Hf_2GeC	
Ge	Zr	Hf	42.4	-12.5	$ZrGe_2$, HfC, ZrC	
Ge	V	Mo	42.6	-12.3	$MoGe_2$, V_2GeC, V_6C_5, Mo_3Ge	
Ge	Mn	Cr	43.1	-11.7	MnGe, C, Cr_3C_2, Mn_3GeC	
Ge	V	Mn	43.7	-11.2	MnGe, V_2GeC, V_6C_5, Ge	
Ge	Mo	Nb	44.1	-10.8	MoC, $MoGe_2$, Mo_3Gw, Nb_6C_5	
Ge	Mo	Zr	45.1	-9.8	ZrC, $MoGe_2$, Mo_2C, Mo_3Ge	
Ge	Ti	Zr	48.7	-6.2	ZrGe, Ti_3GeC_2, ZrC	
Ge	Sc	Hf	50.8	-4.1	ScGe, HfC, Sc_3GeC, C	
Ge	Ta	Zr	51.2	-3.7	Ta_4C_3, ZrGe, $ZrGe_2$	
Ge	Hf	Sc	52.3	-2.6	ScGe, HfC, Hf_2GeC,	
Ge	Ti	Sc	52.7	-2.1	ScGe, Ti_4GeC_3	
Ge	Nb	Cr	53.2	-1.6	Nb_2GeC, $NbGe_2$, Cr_3C_2	
Ge	Mo	V	54.4	-0.5	$MoGe_2$, Mo_2C, V_6C_5, C	
In	Nb	Sc	-15.5	-70.4	Nb_2InC, $ScIn_2$, Sc_3InC, Nb_6C_5	
In	Nb	Ti	-12.9	-67.7	Nb_2InC, Ti_2InC	
In	Ti	Nb	-11.9	-66.8	Ti_2InC, Nb_2InC	
In	Nb	Hf	-4.9	-59.8	Nb_2InC, Hf_2InC	
In	Ti	Ta	-3.5	-58.3	Ti_2InC, Ta_2C, In	
In	Hf	Nb	-2.6	-57.5	Hf_2InC, Nb_2INC	
In	Nb	Zr	-2.5	-57.3	Nb_2InC, Zr_2InC	
In	Zr	Nb	-0.2	-55.0	Zr_2InC, Nb_2InC	
In	Sc	Mo	0.2	-54.6	$(Mo_{2/3}Sc_{1/3})_2InC$, Sc_2MoInC_2, Sc_3InC, $ScIn_3$	
In	Zr	Hf	0.5	-54.4	Zr_2InC, Hf_2InC	
In	Hf	Zr	0.5	-54.3	Hf_2InC, Zr_2InC	
In	Ti	V	2.1	-52.8	Ti_2InC, V_2C, In	
In	Sc	Nb	3.0	-51.9	Sc_3InC, $ScIn_3$, Nb_6C_5, C	
In	V	Ti	7.0	-47.8	V_2C, In, Ti_2InC	
In	Ti	Mo	15.0	-39.9	In, Ti_3InC_2, Mo, Mo_2C	
In	Hf	Ta	15.6	-39.2	Hf_2InC, Ta_2C, In	
In	Sc	Ta	15.7	-39.1	TaC, Sc_3InC, $ScIn_3$, Ta_4C_3	
In	Zr	Ta	16.2	-38.7	Zr_2InC, Ta_2C, In	
In	**Hf**	**Ti**	17.1	-37.8	Hf_2InC, Ti_2InC	synthesized
In	**Ti**	**Hf**	17.3	-37.5	Ti_2InC, Hf_2InC	synthesized
In	Ta	Ti	18.1	-36.7	Ta_2C, In, Ti_2InC	
In	Nb	Ta	20.5	-34.4	Nb_2InC, Ta_2C, In	
In	Nb	V	24.0	-30.9	Nb_2InC, V_2C, In	
In	Zr	Sc	26.6	-28.2	Zr_2InC, ZrC, $ScIn_2$, Sc_3InC	
In	V	Nb	27.5	-27.3	V_2C, In, Nb_2InC	
In	**Zr**	**Ti**	28.8	-26.1	Zr_2InC, Ti_2InC	synthesized
In	**Ti**	**Zr**	29.4	-25.4	Ti_2InC, Zr_2InC	synthesized
In	Ta	Sc	30.4	-24.4	$ScIn_2$, Ta_4C_3, Ta_2C, Sc_3InC	
In	Mo	Sc	36.6	-18.3	$(Sc_{2/3}Mo_{1/3})_2InC$, Mo_2C, In	
In	Ta	Hf	36.8	-18.0	Ta_2C, In, Hf_2InC	
In	Ta	Zr	37.4	-17.4	Ta_2C, In, Zr_2InC	
In	Zr	Mo	38.7	-16.1	ZrC, In, Mo, Zr_2InC	
In	Hf	Sc	39.0	-15.9	Hf_2InC, HfC, Sc_3InC, $ScIn_2$	
In	Mo	Ti	39.9	-14.9	In, Mo_2C, Ti_3InC_2, Mo	
In	V	Ta	40.0	-14.9	In, V_2C, Ta_2C	
In	Ta	Nb	44.1	-10.8	Ta_2C, In, Nb_2InC	
In	Sc	Zr	49.9	-4.9	ZrC, $ScIn_2$, Sc_3InC	
In	Hf	V	52.2	-2.7	Hf_2InC, V_2C, In	
In	Nb	Mo	52.5	-2.3	In, Mo, Nb_2InC, Nb_6C_5	
Pd	V	Cr	36.5	-18.3	VPd_3, V_6C_5, $Cr_{23}C_6$, Cr	
Pd	Cr	V	39.9	-15.0	VPD_3, Cr_3C_2, Cr7C3, V_6C_5	
Pd	Ti	V	42.4	-12.5	$TiC_{0.75}$, $TiPd_2$, V_2C, $TiC_{0.875}$	
Pd	Ti	Ta	43.7	-11.1	$TiPd_2$, $TiC_{0.75}$, Ta_2C, $TiC_{0.875}$	
Pd	Ti	Nb	46.8	-8.1	$TiC_{0.75}$, $TiPd_2$, $TiC_{0.875}$, Nb_2C	
Pd	V	Mo	47.8	-7.1	VPd_3, Mo, Mo_2C, V_6C_5	
Pt	V	Cr	14.5	-40.4	VPt_2, V_6C_5, Cr7C3, Cr_3C_2	
Pt	Cr	V	23.6	-31.3	VPt_2, Cr_3C_2, V_6C_5, Cr7C3	
Pt	V	W	46.1	-8.7	WPt_2, W, V_6C_5, VPt_2	
Pt	V	Ta	54.2	-0.6	$TaPt_2$, V_2C, V_6C_5, Ta_2C	
Si	Ti	Ta	-0.2	-55.1	Ti_3SiC_2, $TaSi_2$, Ta_5Si_3, Ta_4C_3	

Si	V	Ti	11.4	-43.5	VSi_2, Ti_3SiC_2, V_6C_5, V_5Si_3
Si	Ta	Ti	14.6	-40.3	$TaSi_2$, Ti_3SiC_2, Ta_4C_3, TA_5Si_3
Si	Ti	V	20.4	-34.5	Ti_3SiC_2, VSi_2, V_5Si_3, V_6C_5
Si	Ta	Sc	22.4	-32.4	TaC, $TaSi_2$, $Sc_5Si_3C_{0.5}$, Ta_4C_3
Si	Sc	Ta	32.2	-22.7	TaC, $Sc_5Si_3C_{0.5}$, SiC
Si	V	Ta	41.0	-13.8	VSi_2, Ta_4C_3, V_6C_5, V_5Si_3
Si	Ti	W	52.7	-2.1	Ti_4SiC_3, WSi_2, W
Sn	Sc	Nb	-20.5	-75.4	$ScSn_2$, Sc_2SnC, Sc_3SnC, Nb_6C_5
Sn	Zr	Sc	-16.1	-70.9	Zr_2SnC, ZrC, $ScSn_2$, Sc_3SnC
Sn	Sc	Zr	-13.1	-67.9	ZrC, $ScSn_2$, Sc_3SnC
Sn	Nb	Ti	-2.2	-57.1	Nb_2SnC, Ti_2SnC
Sn	Nb	Sc	-2.1	-56.9	$(Sc_{2/3}Nb_{1/3})_2SnC$, Nb_2SnC
Sn	Ti	Nb	-1.9	-56.7	Ti_2SnC, Nb_2SnC
Sn	Zr	Hf	-0.2	-55.1	Zr_2SnC, Hf_2SnC
Sn	Hf	Zr	-0.2	-55.0	Hf_2SnC, Zr_2SnC
Sn	Sc	Ta	0.0	-54.9	TaC, $ScSn_2$, Sc_3SnC
Sn	Hf	Nb	5.6	-49.2	Hf_2SnC, Nb_2SnC
Sn	Nb	Hf	6.5	-48.4	Nb_2nC, Hf_2SnC
Sn	Zr	Nb	7.6	-47.3	Zr_2SnC, Nb_2SnC
Sn	Nb	Zr	8.4	-46.5	Nb_2SnC, Zr_2SnC
Sn	Sc	Mo	12.4	-42.4	Sc_2MoSnC_2, $ScSn_2$, Mo, Sc_3SnC
Sn	Hf	Sc	12.8	-42.1	HfC, Hf_2SnC, Sc_6Sn_5, $ScSn_2$
Sn	Hf	Ti	16.3	-38.6	Hf_2SnC, Ti_2SnC
Sn	Ti	Hf	17.3	-37.6	Ti_2SnC, Hf_2SnC
Sn	Ti	V	19.1	-35.7	Ti_2SnC, V_2C, Sn
Sn	Sc	Ti	19.5	-35.4	Sc_2SnC, Ti_3SnC_2, $ScSn_2$, Sc_3SnC
Sn	Ti	Ta	19.6	-35.3	Ti_2SnC, Ta_2C, Sn
Sn	V	Ti	19.9	-34.9	V_2C, Sn, Ti_2SnC
Sn	Nb	V	24.2	-30.6	Nb_2SnC, V_2C, Sn
Sn	Sc	Hf	25.2	-29.6	HfC, $ScSn_2$, Sc_3SnC
Sn	Zr	Ti	28.6	-26.2	Zr_2SnC, Ti_2SnC
Sn	Ti	Sc	28.9	-26.0	Ti_3SnC_2, $ScSn_2$, Sc_3SnC, Sc_6Sn_5
Sn	Ti	Zr	30.1	-24.8	Ti_2SnC, Zr_2SnC
Sn	V	Nb	31.0	-23.8	V_2C, Sn, Nb_2SnC
Sn	Ti	Mo	31.8	-23.1	Sn, Ti_3SnC_2, Mo, Mo_2C
Sn	Nb	Ta	32.5	-22.3	Nb_2SnC, Ta_2C, Sn
Sn	Hf	Ta	36.8	-18.0	Hf_2SnC, Ta_2C, Sn
Sn	Zr	Ta	38.4	-16.5	Zr_2SnC, $ZrSn_2$, Ta_2C, Ta_4C_3
Sn	Zr	Mo	53.4	-1.5	Zr_2SnC, Mo_2C, Sn
Sn	V	Ta	54.7	-0.1	Sn, V_2C, Ta_2C
Sn	Ta	Ti	54.8	-0.1	Ta_2C, Sn, Ti_2SnC
Zn	V	Ti	15.4	-39.4	V_2ZnC, Ti_3Zn_3C, TiC, V_2C
Zn	Mn	Fe	15.5	-39.4	C, Fe, $FeZn_{13}$, $Mn_{23}C_6$
Zn	Ti	V	25.4	-29.4	V_2C, TiC, Ti_3Zn_3C
Zn	Ti	Nb	29.3	-25.5	$TiC_{0.875}$, Nb_2C, Ti_3Zn_3C, $NbZn_3$
Zn	Fe	Mn	29.6	-25.2	$FeZn_{13}$, $Mn_{23}C_6$
Zn	Nb	Ti	33.1	-21.7	Nb_2C, $TiC_{0.875}$, $NbZn_3$, Ti_3Zn_3C
Zn	Mn	Cr	33.9	-21.0	Zn, Cr_3C_2, C, $Mn_{23}C_6$
Zn	V	Ta	35.4	-19.5	V_2ZnC, Ta_2C, Zn
Zn	Ti	Ta	36.9	-17.9	TiC, Ti_3Zn_3C, Ta_2C
Zn	Ti	Mo	41.9	-12.9	TiC, Mo, Ti_3Zn_3C, $MoZn_6$
Zn	Mn	Co	43.8	-11.0	C, Co_3ZnC, $CoZn_{13}$, $Mn_{23}C_6$,
Zn	Ta	Ti	44.4	-10.5	Ta_2C, TiC, $TiZn_3$
Zn	V	Cr	47.5	-7.4	Zn, Cr, V_2ZnC, V_6C_5
Zn	Nb	Ta	51.6	-3.2	$NbZn_3$, Ta_2C, Nb_2C, Nb_6C_5
Zn	Nb	V	52.5	-2.3	$NbZn_3$, V_2C, Nb_2C, Nb_6C_5
Zn	Cr	Mn	53.3	-1.5	Cr_3C_2, Zn, $MnZn_3$, $Mn_{23}C_6$

Supplementary Table 6. Statistics of the known and predicted quaternary *i*-MAX phases and solid solution MAX phases, categorized by the calculated thermodynamic stability, $\Delta H_{i\text{-MAX}}$ or $\Delta G_{\text{solid solution}}$, and energy difference between order and solid solution phases, $\Delta H_{i\text{-MAX}}$ - $\Delta G_{\text{solid solution}}$, at 2000 K. Metastable phases are categorized by their formation enthalpy above the convex hull. Units is in meV/atom.

Quaternary $(M'_{2/3}M''_{1/3})_2AC$ phases	**Stability criteria**		**Previously known**	**Newly Predicted**
	$\Delta H_{i\text{-MAX}}$ or $\Delta G_{\text{solid solution}}$	$\Delta H_{i\text{-MAX}}$ - $\Delta G_{\text{solid solution}}$		
Stable *i*-MAX	$\Delta H_{i\text{-MAX}} < 0$	< 0	13	79
Nonstable or metastable *i*-MAX	$0 \le \Delta H_{i\text{-MAX}} \le +60$ meV/atom	< 0	0	163
Stable solid solution MAX	$\Delta G_{\text{solid solution}} < 0$	> 0	34	257
Nonstable or metastable solid solution MAX	$0 \le \Delta G_{\text{solid solution}} \le +60$ meV/atom	> 0	1	255

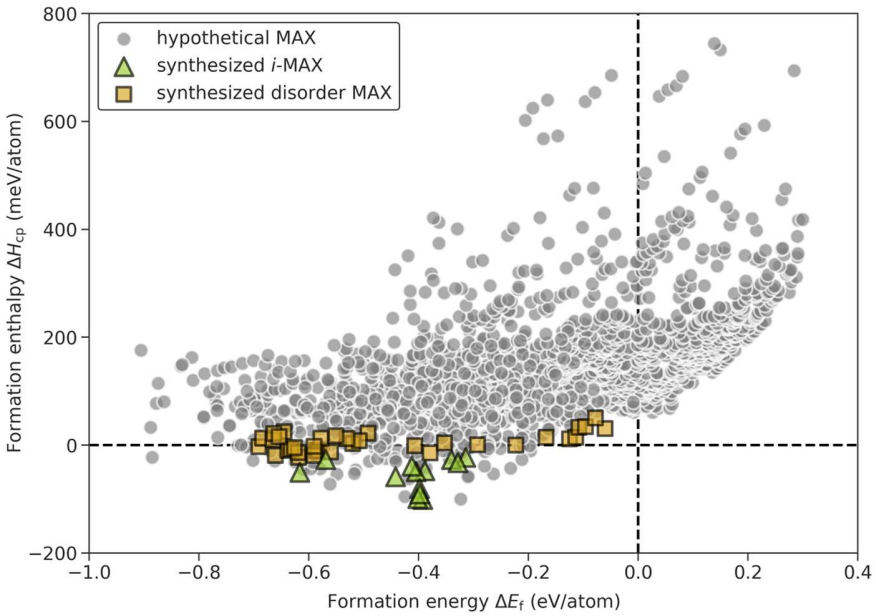

Supplementary Fig. 3. Calculated formation enthalpy as function of formation energy for $(M'_{2/3}M''_{1/3})_2AC$ phases. Experimentally reported *i*-MAX phases are represented by green triangles and MAX with disorder by orange squares.

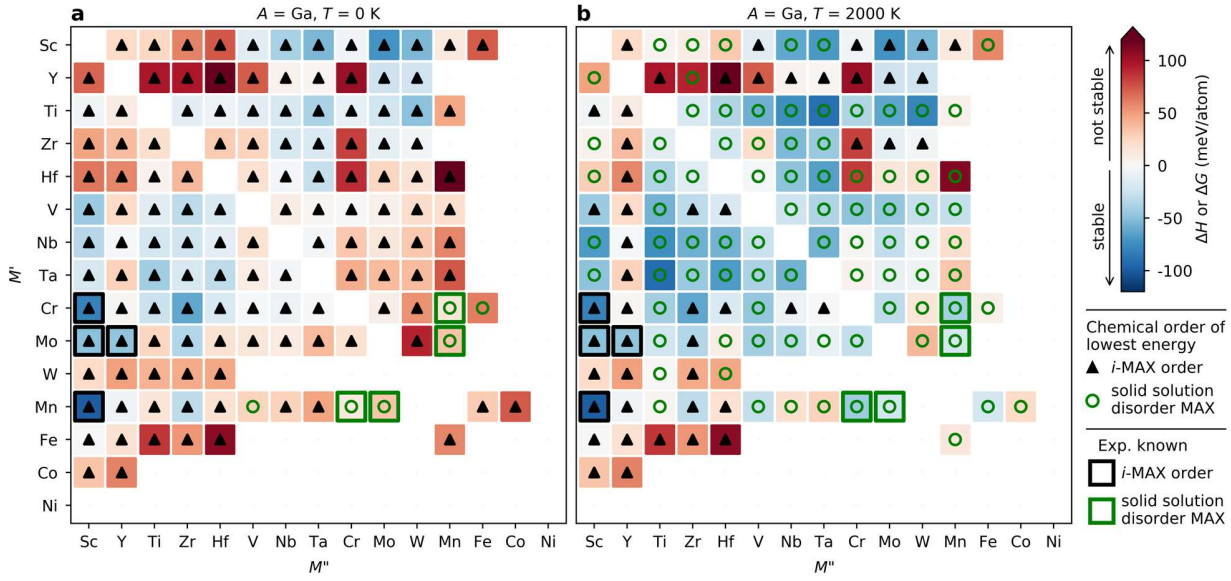

Supplementary Fig. 4. Calculated formation enthalpy ΔH and Gibbs free energy of formation ΔG at (a) 0 K and (b) 2000 K for $(M'_{2/3}M''_{1/3})_2$GaC. Symbols represent chemical order of lowest energy at given M' and M'' with *i*-MAX represented by black triangles or solid solution MAX by green circles. Experimentally reported phases are marked by green (*i*-MAX) or black (solid solution MAX) squares.

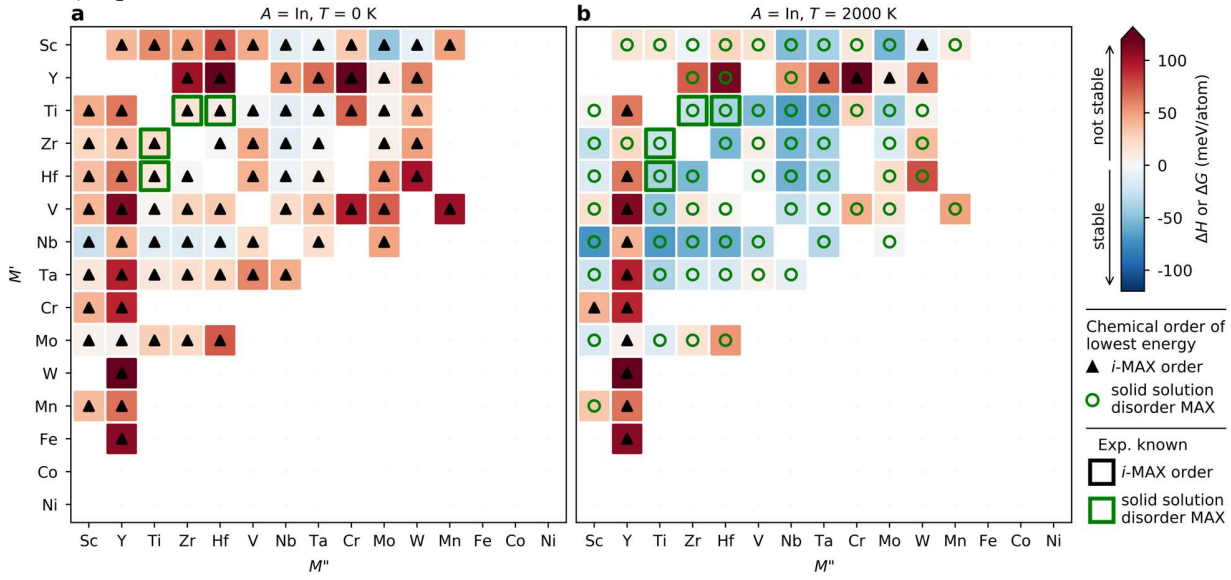

Supplementary Fig. 5. Calculated formation enthalpy ΔH and Gibbs free energy of formation ΔG at (a) 0 K and (b) 2000 K for $(M'_{2/3}M''_{1/3})_2$InC. Symbols represent chemical order of lowest energy at given M' and M'' with *i*-MAX represented by black triangles or solid solution MAX by green circles. Experimentally reported phases are marked by green (*i*-MAX) or black (solid solution MAX) squares.

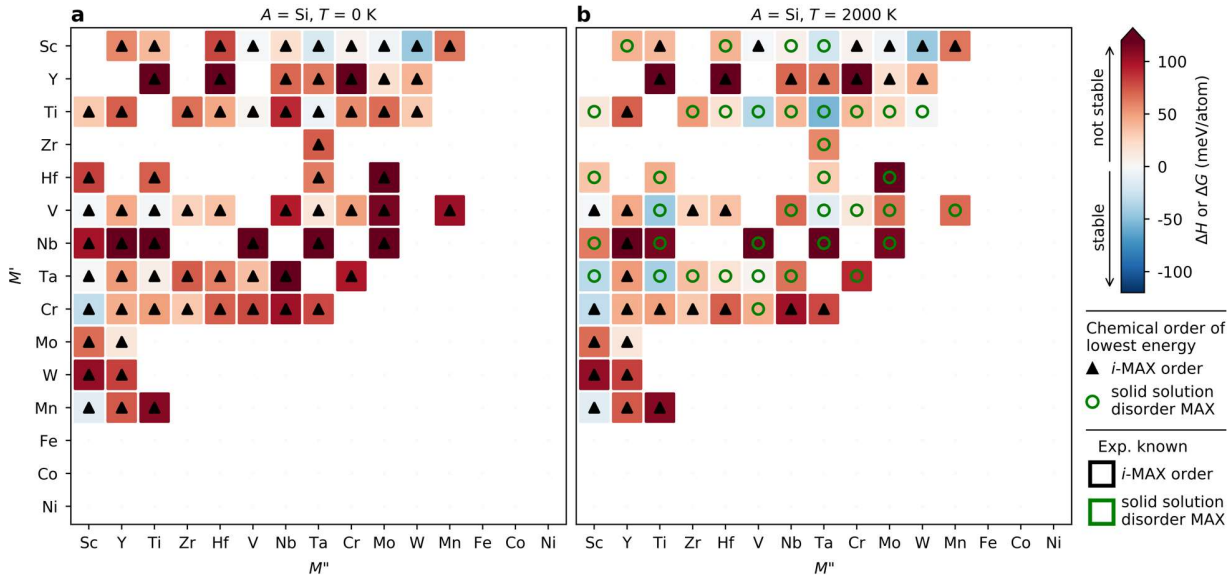

Supplementary Fig. 6. Calculated formation enthalpy ΔH and Gibbs free energy of formation ΔG at (a) 0 K and (b) 2000 K for $(M'_{2/3}M''_{1/3})_2$SiC. Symbols represent chemical order of lowest energy at given M' and M'' with *i*-MAX represented by black triangles or solid solution MAX by green circles. Experimentally reported phases are marked by green (*i*-MAX) or black (solid solution MAX) squares.

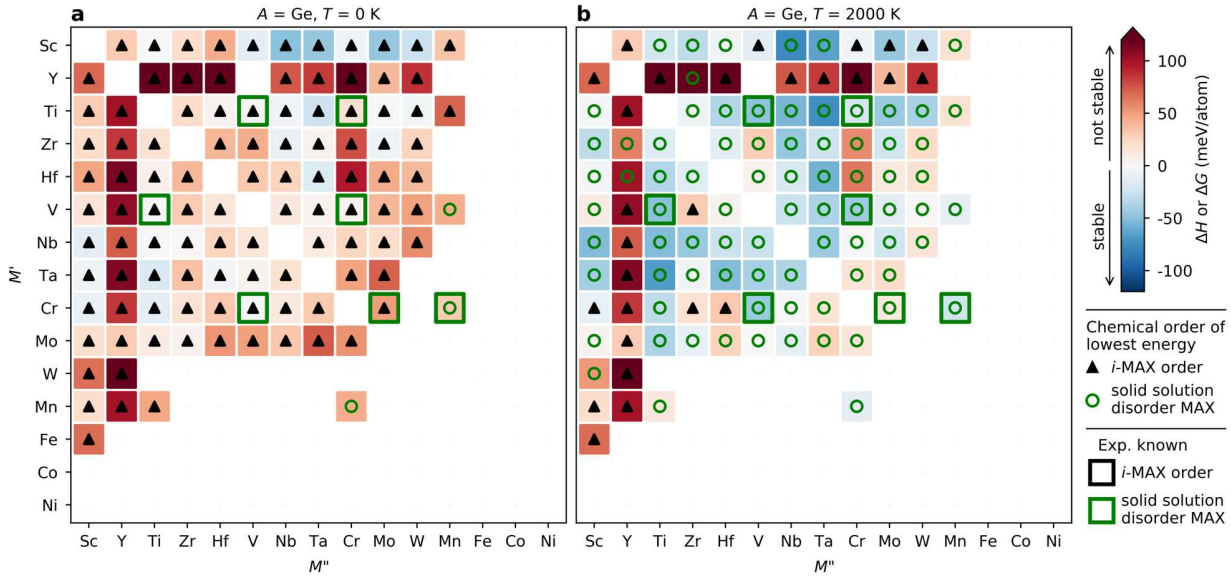

Supplementary Fig. 7. Calculated formation enthalpy ΔH and Gibbs free energy of formation ΔG at (a) 0 K and (b) 2000 K for $(M'_{2/3}M''_{1/3})_2$GeC. Symbols represent chemical order of lowest energy at given M' and M'' with *i*-MAX represented by black triangles or solid solution MAX by green circles. Experimentally reported phases are marked by green (*i*-MAX) or black (solid solution MAX) squares.

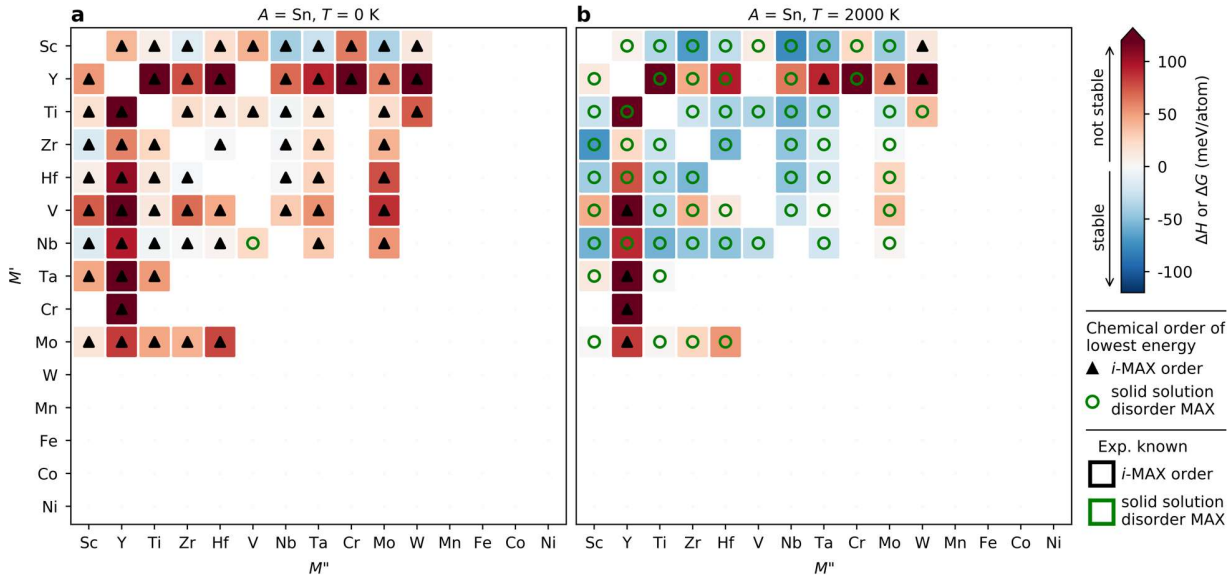

Supplementary Fig. 8. Calculated formation enthalpy ΔH and Gibbs free energy of formation ΔG at (a) 0 K and (b) 2000 K for $(M'_{2/3}M''_{1/3})_2$SnC. Symbols represent chemical order of lowest energy at given M' and M'' with *i*-MAX represented by black triangles or solid solution MAX by green circles. Experimentally reported phases are marked by green (*i*-MAX) or black (solid solution MAX) squares.

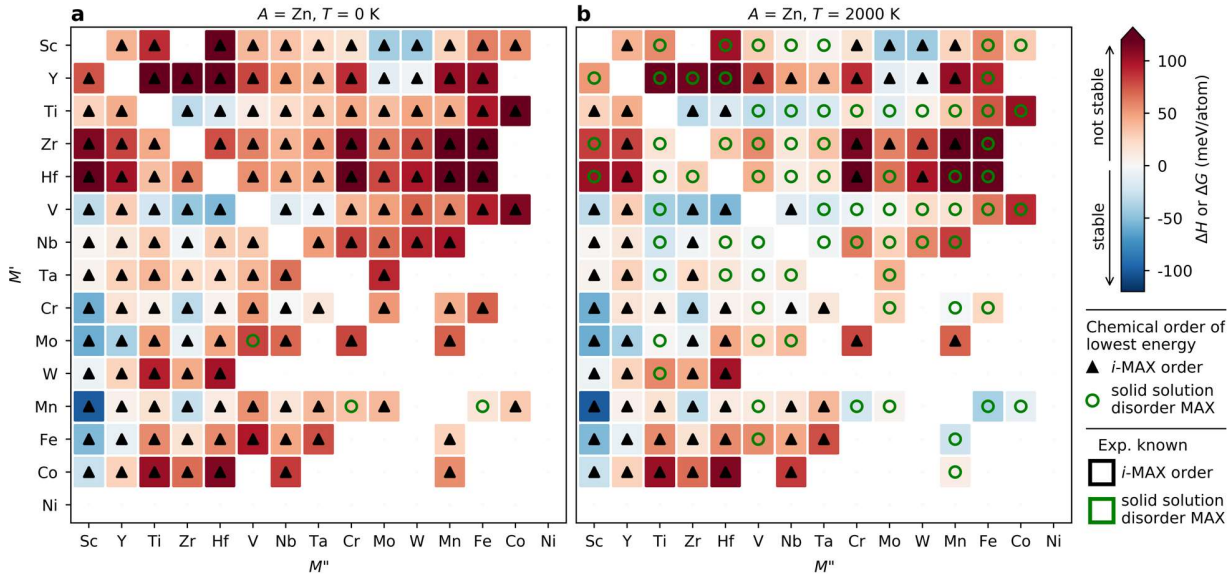

Supplementary Fig. 9. Calculated formation enthalpy ΔH and Gibbs free energy of formation ΔG at (a) 0 K and (b) 2000 K for $(M'_{2/3}M''_{1/3})_2$ZnC. Symbols represent chemical order of lowest energy at given M' and M'' with *i*-MAX represented by black triangles or solid solution MAX by green circles. Experimentally reported phases are marked by green (*i*-MAX) or black (solid solution MAX) squares.

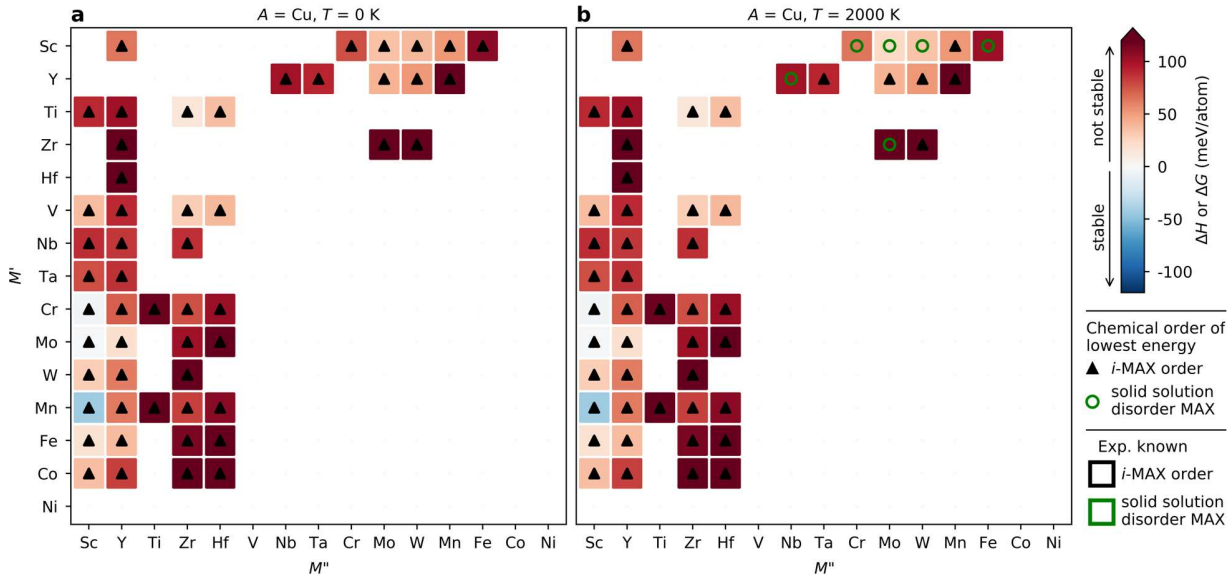

Supplementary Fig. 10. Calculated formation enthalpy ΔH and Gibbs free energy of formation ΔG at (a) 0 K and (b) 2000 K for $(M'_{2/3}M''_{1/3})_2$CuC. Symbols represent chemical order of lowest energy at given M' and M'' with *i*-MAX represented by black triangles or solid solution MAX by green circles. Experimentally reported phases are marked by green (*i*-MAX) or black (solid solution MAX) squares.

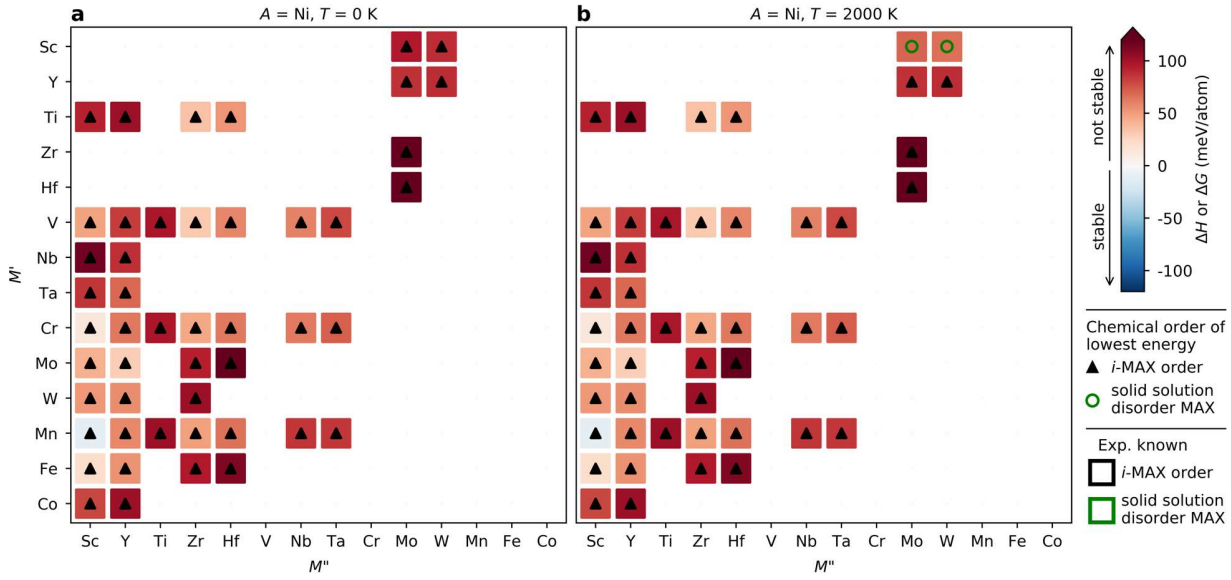

Supplementary Fig. 11. Calculated formation enthalpy ΔH and Gibbs free energy of formation ΔG at (a) 0 K and (b) 2000 K for $(M'_{2/3}M''_{1/3})_2$NiC. Symbols represent chemical order of lowest energy at given M' and M'' with *i*-MAX represented by black triangles or solid solution MAX by green circles. Experimentally reported phases are marked by green (*i*-MAX) or black (solid solution MAX) squares.

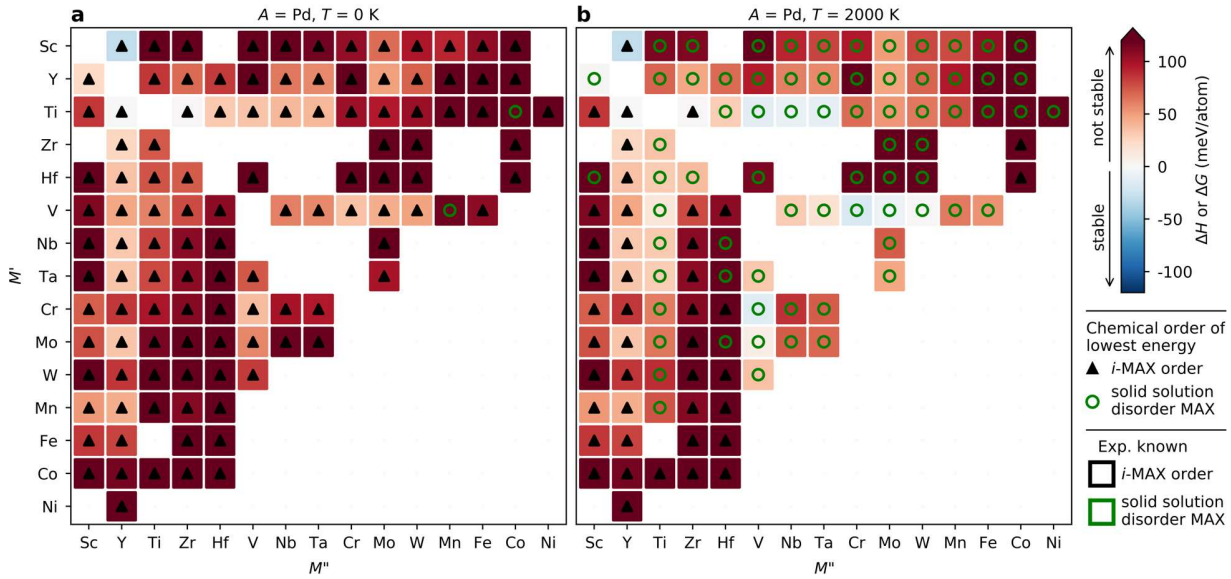

Supplementary Fig. 12. Calculated formation enthalpy ΔH and Gibbs free energy of formation ΔG at (a) 0 K and (b) 2000 K for $(M'_{2/3}M''_{1/3})_2$PdC. Symbols represent chemical order of lowest energy at given M' and M'' with *i*-MAX represented by black triangles or solid solution MAX by green circles. Experimentally reported phases are marked by green (*i*-MAX) or black (solid solution MAX) squares.

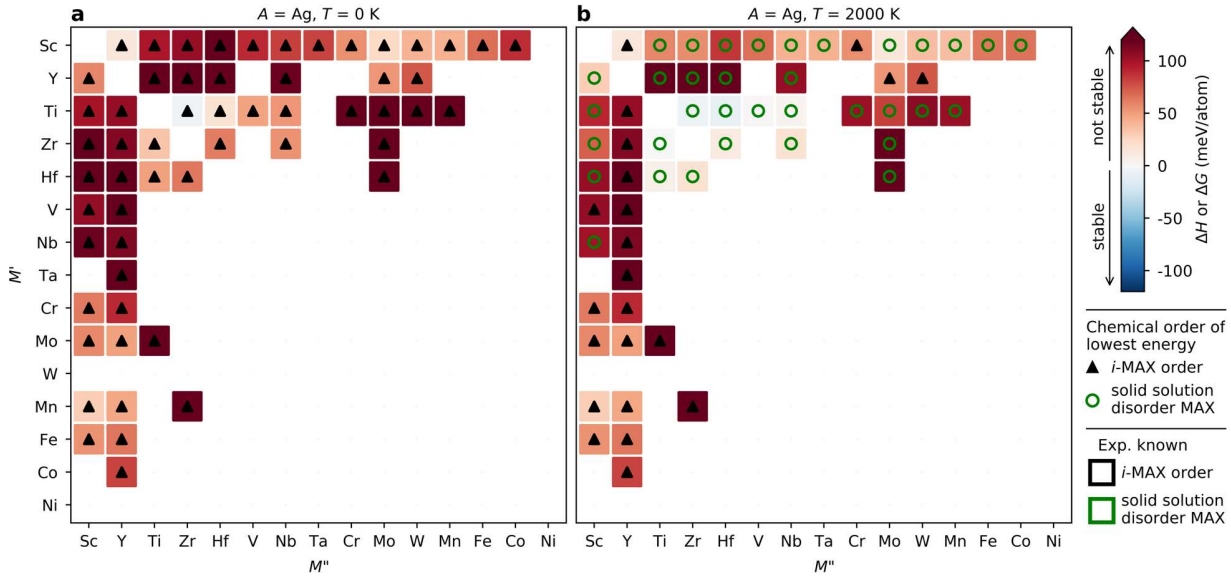

Supplementary Fig. 13. Calculated formation enthalpy ΔH and Gibbs free energy of formation ΔG at (a) 0 K and (b) 2000 K for $(M'_{2/3}M''_{1/3})_2$AgC. Symbols represent chemical order of lowest energy at given M' and M'' with *i*-MAX represented by black triangles or solid solution MAX by green circles. Experimentally reported phases are marked by green (*i*-MAX) or black (solid solution MAX) squares.

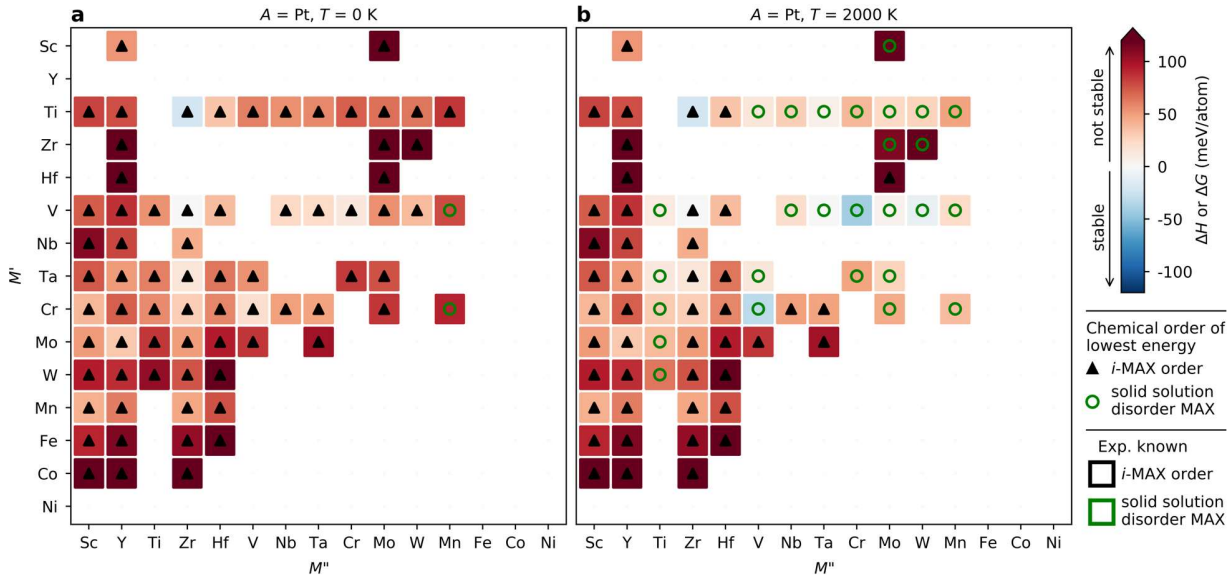

Supplementary Fig. 14. Calculated formation enthalpy ΔH and Gibbs free energy of formation ΔG at (a) 0 K and (b) 2000 K for $(M'_{2/3}M''_{1/3})_2$PtC. Symbols represent chemical order of lowest energy at given M' and M'' with *i*-MAX represented by black triangles or solid solution MAX by green circles. Experimentally reported phases are marked by green (*i*-MAX) or black (solid solution MAX) squares.

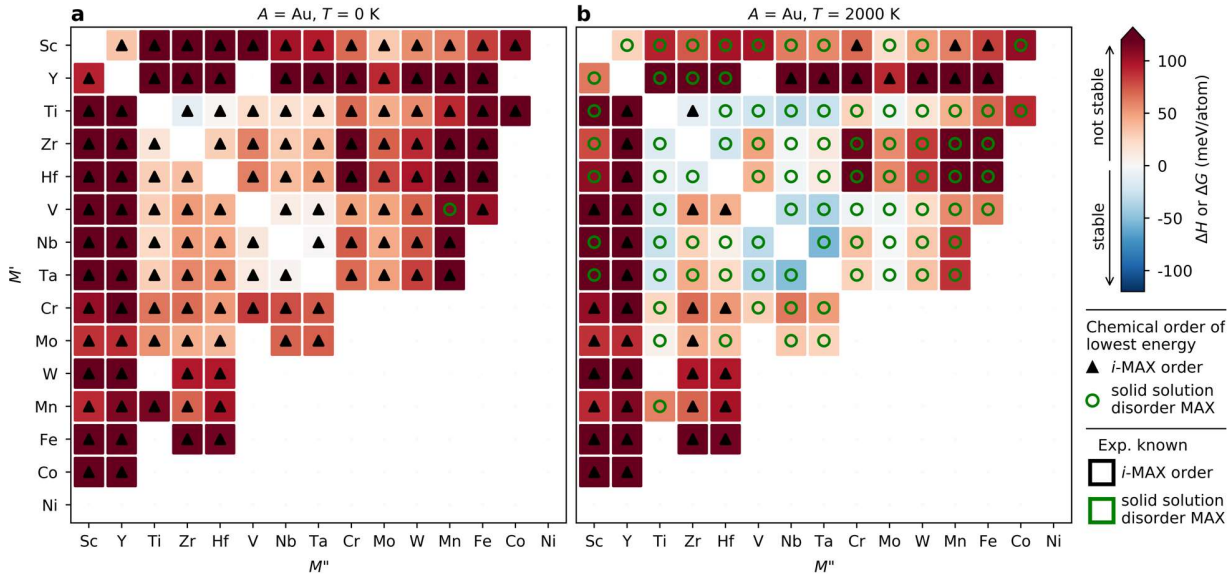

Supplementary Fig. 15. Calculated formation enthalpy ΔH and Gibbs free energy of formation ΔG at (a) 0 K and (b) 2000 K for $(M'_{2/3}M''_{1/3})_2$AuC. Symbols represent chemical order of lowest energy at given M' and M'' with *i*-MAX represented by black triangles or solid solution MAX by green circles. Experimentally reported phases are marked by green (*i*-MAX) or black (solid solution MAX) squares

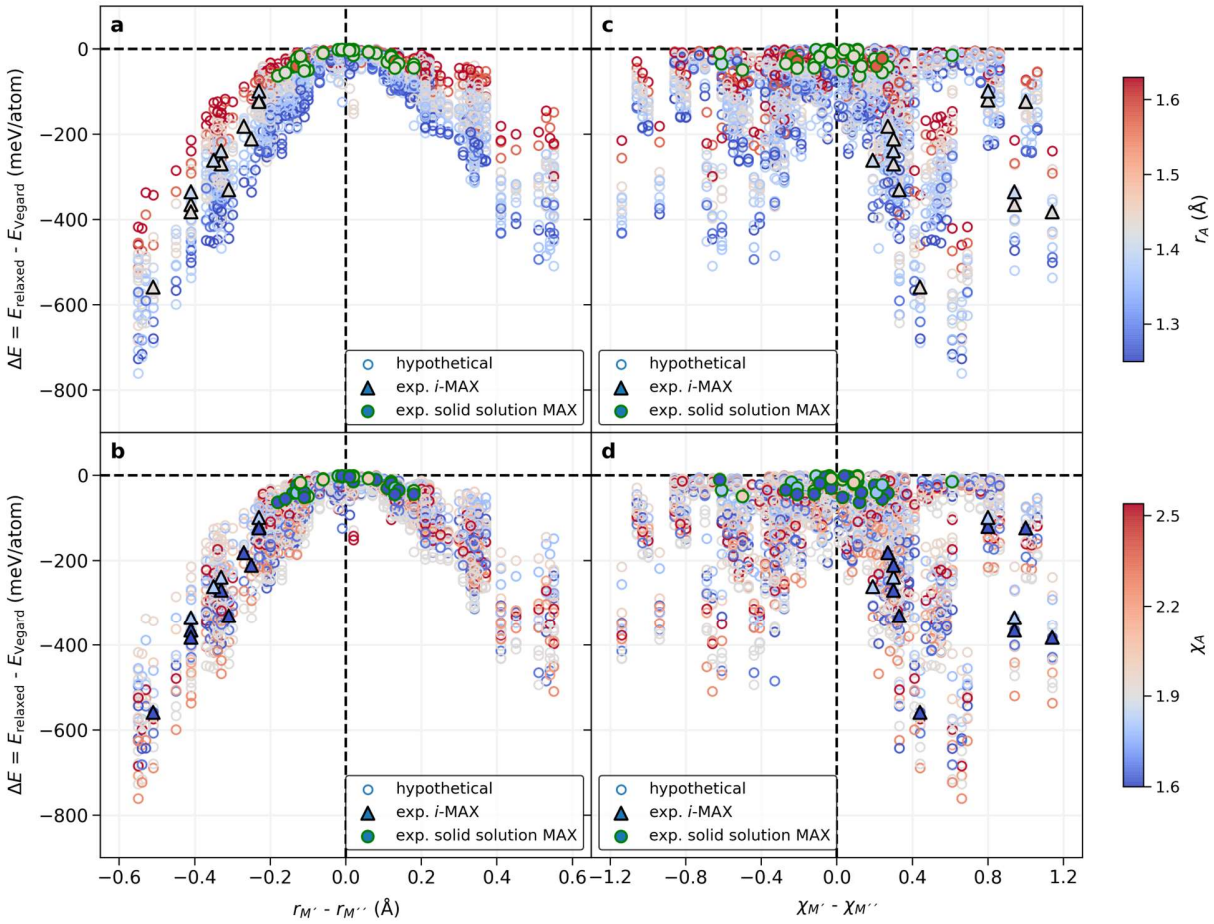

Supplementary Fig. 16. Calculated energy difference between relaxed *i*-MAX and MAX phase generated by Vegard's law structure as function of **a,b** atomic size difference of M' and M'' and *c,d* electronegativity difference of M' and M''. Experimentally known *i*-MAX phases are indicated by black triangles and solid solution MAX phases by green circles. The coloring represents the atomic radius (a,c) or electronegativity (b,d) of the *A* element.

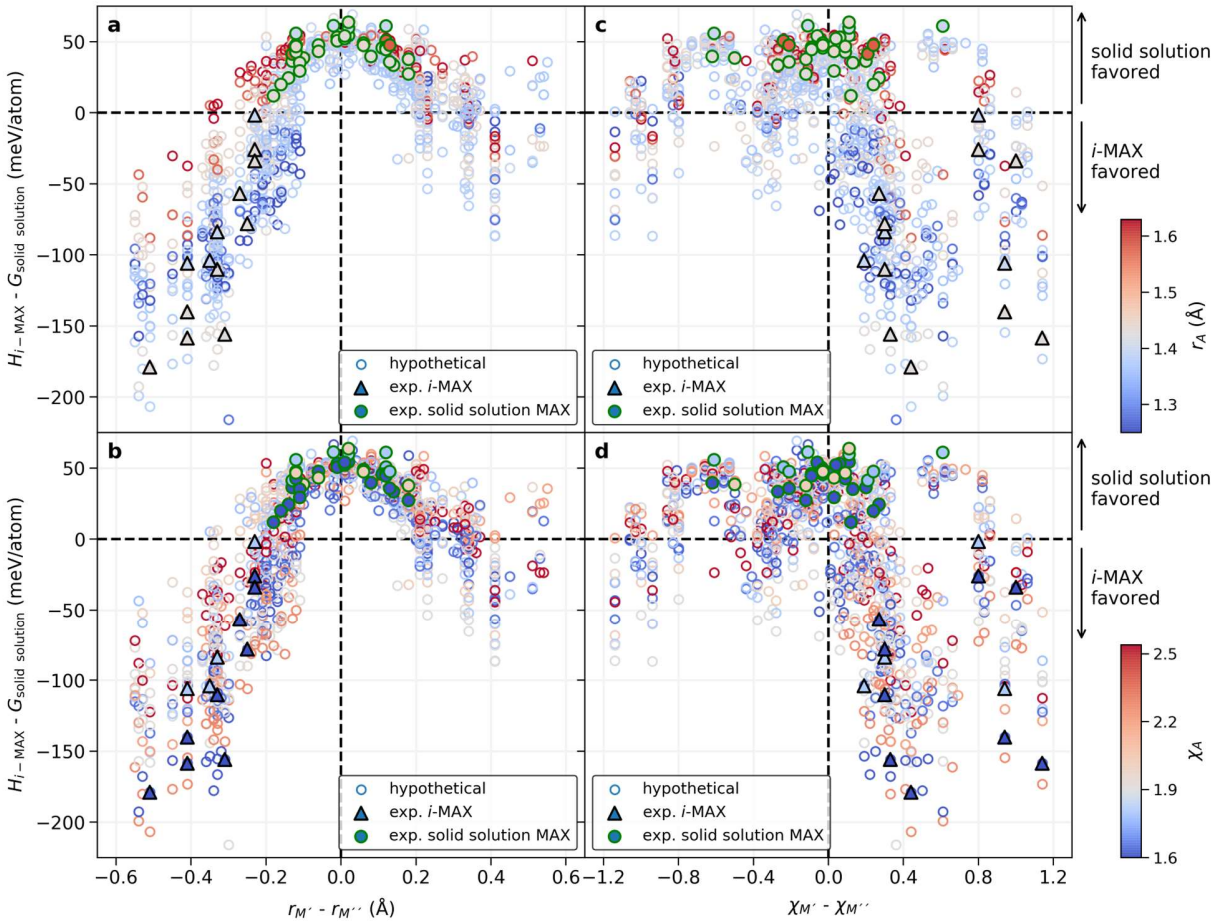

Supplementary Fig. 17. Energy difference between *i*-MAX and solid solution MAX at 2000 K as function of **a,b** atomic size difference of *M′* and *M′′* and **c,d** electronegativity difference of *M′* and *M′′*. Experimentally known *i*-MAX phases are indicated by black triangles and solid solution MAX phases by green circles. The coloring represents the atomic radius (a,c) or electronegativity (b,d) of the *A* element.

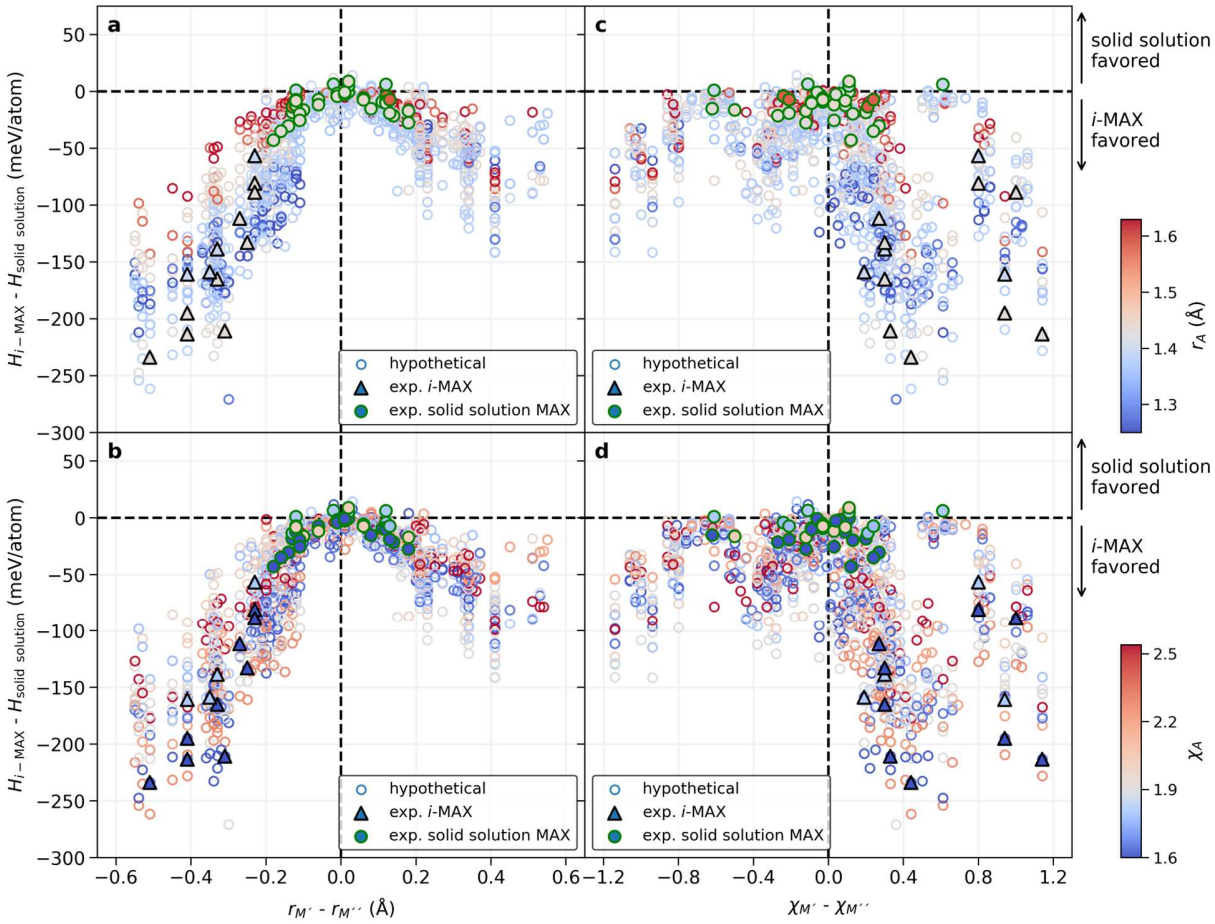

Supplementary Fig. 18. Energy difference between *i*-MAX and solid solution MAX at 0 K as function of **a,b** atomic size difference of M' and M'' and **c,d** electronegativity difference of M' and M''. Experimentally known *i*-MAX phases are indicated by black triangles and solid solution MAX phases by green circles. The coloring represents the atomic radius (a,c) or electronegativity (b,d) of the *A* element.

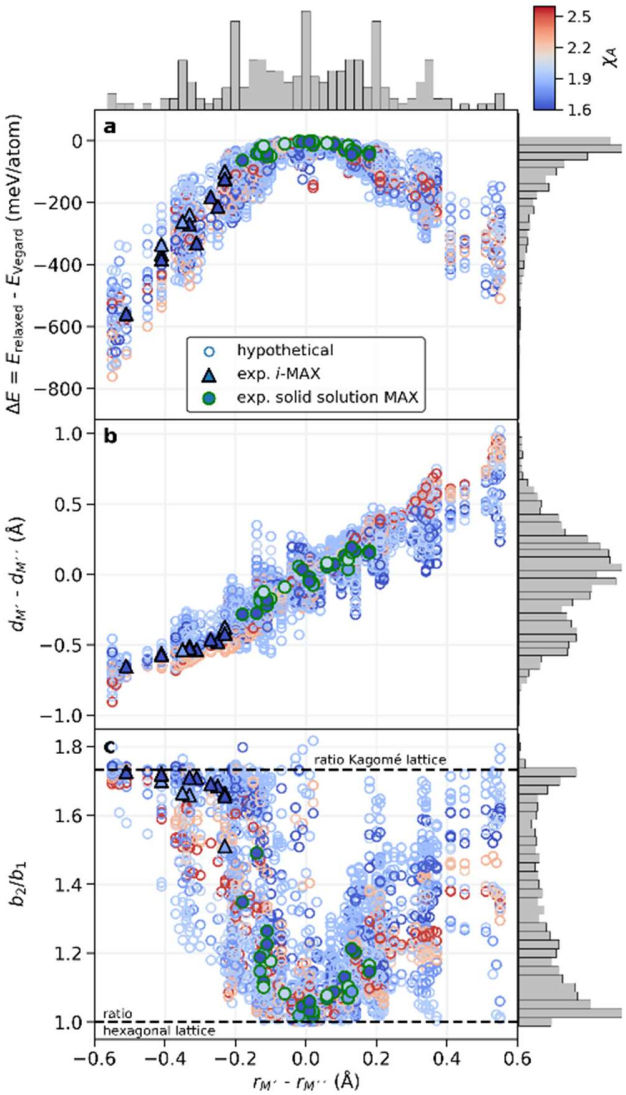

Supplementary Fig. 19. Calculated energy difference between relaxed *i*-MAX and MAX phase generated by Vegard's law structure, **b** interlayer distance between M' and M'' for relaxed *i*-MAX, and **c** ratio of next-nearest and nearest *A*-*A* distance within the *A*-layer, as function of atomic size difference of M' and M'' for $(M'_{2/3}M''_{1/3})_2AC$. Experimentally known *i*-MAX phases are indicated by black triangles and solid solution MAX phases by green circles. The coloring represents the electronegativity of the *A* element. Histograms are given for each axis.

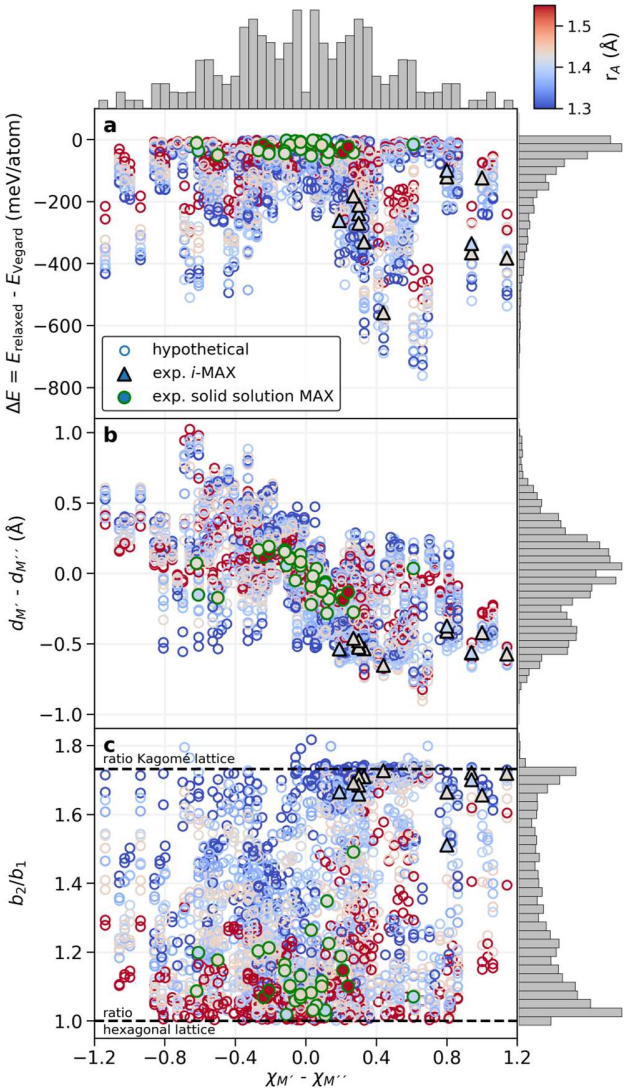

Supplementary Fig. 20. Calculated energy difference between relaxed *i*-MAX and MAX phase generated by Vegard's law structure, **b** interlayer distance between M' and M'' for relaxed *i*-MAX, and **c** ratio of next-nearest and nearest *A*-*A* distance within the *A*-layer, as function of electronegativity difference of M' and M'' for $(M'_{2/3}M''_{1/3})_2AC$. Experimentally known *i*-MAX phases are indicated by black triangles and solid solution MAX phases by green circles. The coloring represents the atomic radius of the *A* element. Histograms are given for each axis.

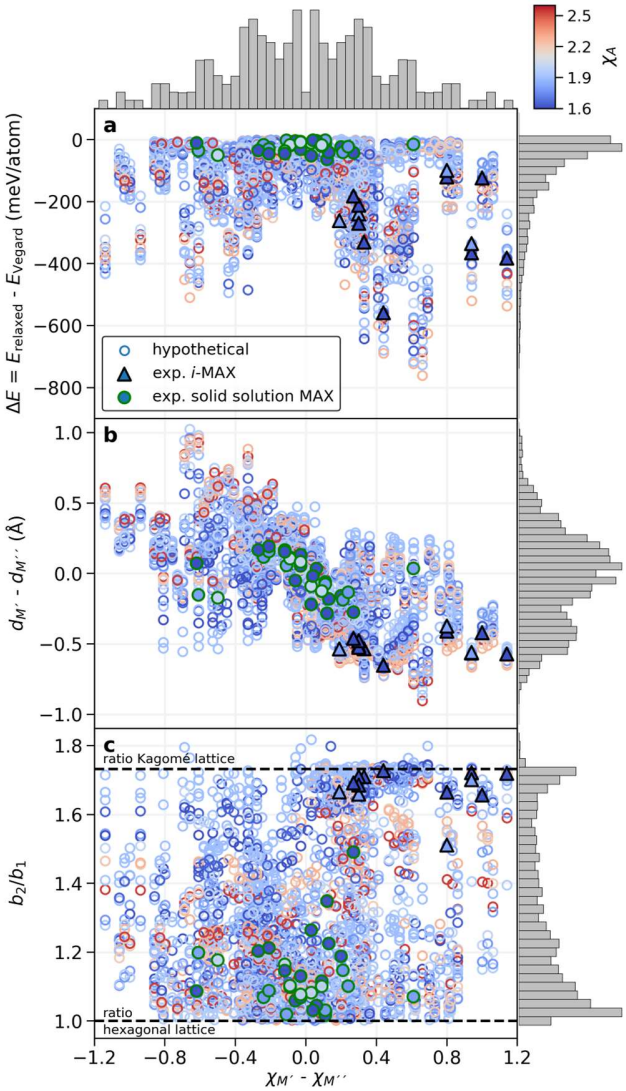

Supplementary Fig. 21. Calculated energy difference between relaxed *i*-MAX and MAX phase generated by Vegard's law structure, **b** interlayer distance between M' and M'' for relaxed *i*-MAX, and **c** ratio of next-nearest and nearest *A*-*A* distance within the *A*-layer, as function of electronegativity difference of M' and M'' for $(M'_{2/3}M''_{1/3})_2AC$. Experimentally known *i*-MAX phases are indicated by black triangles and solid solution MAX phases by green circles. The coloring represents the electronegativity of the *A* element. Histograms are given for each axis.

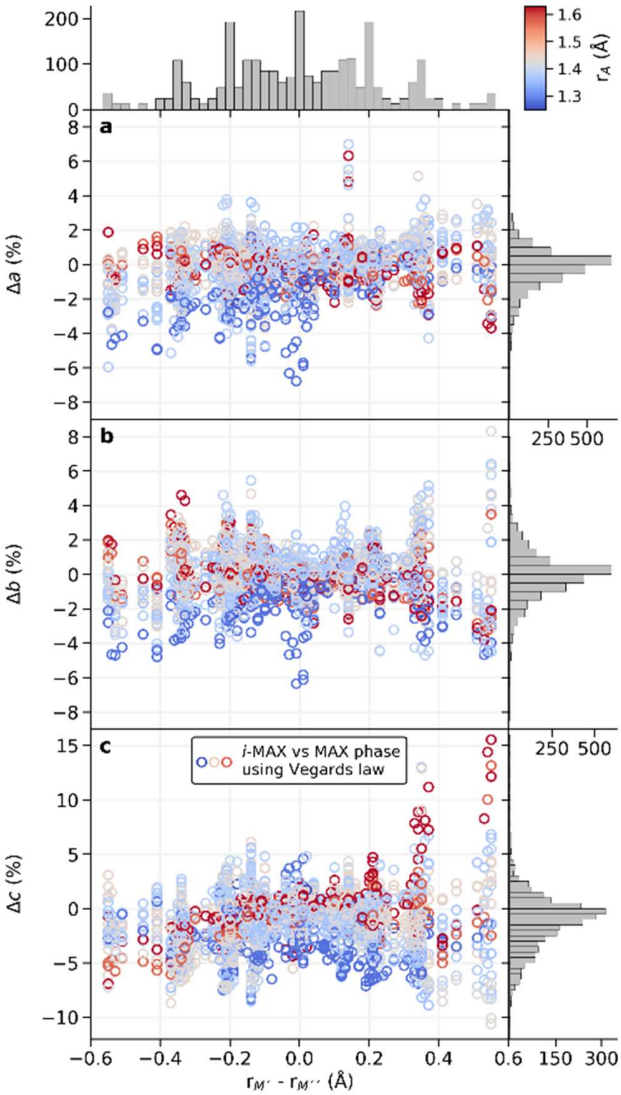

Supplementary Fig. 22. Deviation in lattice parameters *a*, *b* and *c* between the relaxed *i*-MAX structure and the MAX phase structure generated by using Vegard's law as function of atomic size difference of M' and M'' for $(M'_{2/3}M''_{1/3})_2AC$. The coloring represents the atomic radius of the *A* element. Histograms are given for each axis.

Supplementary Table 7. PBE potentials for considered elements in this work.

Element	PBE potential	Valence states
Sc	Sc_sv	3*s*3*p*4*s*3*d*
Y	Y_sv	4*s*4*p*5*s*4*d*
Ti	Ti	4*s*3*d*
Zr	Zr_sv	4*s*4*p*5*s*4*d*
Hf	Hf_pv	5*p*6*s*5*d*
V	V_sv	3*s*3*p*4*s*3*d*
Nb	Nb_pv	4*p*5*s*4*d*
Ta	Ta	6*s*5*d*
Cr	Cr_pv	3*p*4*s*3*d*
Mo	Mo_pv	4*p*5*s*4*d*
W	W	6*s*5*d*
Mn	Mn_pv	3*p*4*s*3*d*
Fe	Fe_pv	3*p*4*s*3*d*
Co	Co	4*s*3*d*
Ni	Ni	4*s*3*d*
Al	Al	3*s*3*p*
Ga	Ga_d	4*s*4*p*3*d*
In	In_d	5*s*5*p*4*d*
Si	Si	3*s*3*p*
Ge	Ge_d	4*s*4*p*3*d*
Sn	Sn_d	5*s*5*p*4*d*
Cu	Cu	4*p*3*d*
Zn	Zn	4*p*3*d*
Pd	Pd_pv	4*p*5*s*4*d*
Ag	Ag	5*s*4*d*
Pt	Pt_pv	5*p*6*s*5*d*
Au	Au	6*s*5*d*
C	C	2*s*2*p*

REFERENCES

1. Schuster J. C., Nowotny H., Vaccaro C. The ternary systems: CrAlC, VAlC, and TiAlC and the behavior of H-phases (M_2AlC). *J Solid State Chem* **32**, 213-219 (1980).
2. Yeh C. L., Yang W. J. Formation of MAX solid solutions $(Ti,V)_2AlC$ and $(Cr,V)_2AlC$ with Al_2O_3 addition by SHS involving aluminothermic reduction. *Ceram Int* **39**, 7537-7544 (2013).
3. Yeh C.-L., Yang W.-J. Effects of Ti and TiO_2 on Combustion Synthesis of $(Ti,V)_2AlC/Al_2O_3$ Solid Solution Composites. *Materials and Manufacturing Processes* **30**, 292-297 (2015).
4. Han M., Maleski K., Shuck C. E., Yang Y., Glazar J. T., Foucher A. C.*, et al.* Tailoring Electronic and Optical Properties of MXenes through Forming Solid Solutions. *J Am Chem Soc* **142**, 19110-19118 (2020).
5. Tian W., Sun Z., Hashimoto H., Du Y. Synthesis, microstructure and properties of $(Cr_{1-x}V_x)_2AlC$ solid solutions. *J Alloys Compd* **484**, 130-133 (2009).
6. Caspi E. N., Chartier P., Porcher F., Damay F., Cabioch T. Ordering of (Cr,V) layers in nanolamellar $(Cr_{0.5}V_{0.5})_{n+1}AlC_n$ compounds. *Mater Res Lett* **3**, 100-106 (2015).
7. Halim J., Chartier P., Basyuk T., Prikhna T., Caspi E. a. N., Barsoum M. W.*, et al.* Structure and thermal expansion of $(Cr_x,V_{1-x})_{n+1}AlC_n$ phases measured by X-ray diffraction. *J Eur Ceram Soc* **37**, 15-21 (2017).
8. Horlait D., Grasso S., Al Nasiri N., Burr P. A., Lee W. E. Synthesis and Oxidation Testing of MAX Phase Composites in the Cr–Ti–Al–C Quaternary System. *J Am Ceram Soc* **99**, 682-690 (2016).
9. Scabarozi T. H., Gennaoui C., Roche J., Flemming T., Wittenberger K., Hann P.*, et al.* Combinatorial investigation of $(Ti_{1-x}Nb_x)_2AlC$. *Appl Phys Lett* **95**, 101907 (2009).
10. Yeh C. L., Chen J. H. Combustion synthesis of $(Ti_{1-x}Nb_x)_2AlC$ solid solutions from elemental and Nb_2O_5/Al_4C_3-containing powder compacts. *Ceram Int* **37**, 3089-3094 (2011).
11. Salama I., El-Raghy T., Barsoum M. W. Synthesis and mechanical properties of Nb_2AlC and $(Ti,Nb)_2AlC$. *J Alloys Compd* **347**, 271-278 (2002).
12. Nowotny H., Rogl P., Schuster J. C. Structural chemistry of complex carbides and related compounds. *J Solid State Chem* **44**, 126-133 (1982).
13. Griseri M., Tunca B., Huang S., Dahlqvist M., Rosén J., Lu J.*, et al.* Ta-based 413 and 211 MAX phase solid solutions with Hf and Nb. *J Eur Ceram Soc* **40**, 1829-1838 (2020).
14. Sridharan S., Nowotny H. Studies in the ternary system Ti-Ta-Al and in the quaternary system Ti-Ta-Al-C. *Z Metallkd* **74**, 468-472 (1983).
15. Tunca B., Lapauw T., Karakulina O. M., Batuk M., Cabioc'h T., Hadermann J.*, et al.* Synthesis of MAX Phases in the Zr-Ti-Al-C System. *Inorg Chem* **56**, 3489-3498 (2017).
16. Zapata-Solvas E., Hadi M. A., Horlait D., Parfitt D. C., Thibaud A., Chroneos A.*, et al.* Synthesis and physical properties of $(Zr_{1-x},Ti_x)_3AlC_2$ MAX phases. *J Am Ceram Soc* **100**, 3393-3401 (2017).
17. Naguib M., Bentzel G. W., Shah J., Halim J., Caspi E. N., Lu J.*, et al.* New Solid Solution MAX Phases: $(Ti_{0.5},V_{0.5})_3AlC_2$, $(Nb_{0.5},V_{0.5})_2AlC$, $(Nb_{0.5},V_{0.5})_4AlC_3$ and $(Nb_{0.8},Zr_{0.2})_2AlC$. *Mater Res Lett* **2**, 233-240 (2014).

18. Schuster J. C., Nowotny H. INVESTIGATIONS OF THE TERNARY SYSTEMS (Zr, Hf, Nb, Ta)-Al-C AND STUDIES ON COMPLEX CARBIDES. *Z Metallkd* **71**, 341-346 (1980).
19. Mockute A., Dahlqvist M., Emmerlich J., Hultman L., Schneider J. M., Persson P. O. Å., *et al.* Synthesis and *ab initio* calculations of nanolaminated $(Cr,Mn)_2AlC$ compounds. *Phys Rev B* **87**, 094113 (2013).
20. Mockute A., Lu J., Moon E. J., Yan M., Anasori B., May S. J., *et al.* Solid solubility and magnetism upon Mn incorporation in the bulk ternary carbides Cr_2AlC and Cr_2GaC. *Mater Res Lett* **3**, 16-22 (2014).
21. Hamm C. M., Bocarsly J. D., Seward G., Kramm U. I., Birkel C. S. Non-conventional synthesis and magnetic properties of MAX phases $(Cr/Mn)_2AlC$ and $(Cr/Fe)_2AlC$. *J Mater Chem C* **5**, 5700-5708 (2017).
22. Reiffenstein E., Nowotny H., Benesovsky F. Strukturchemische und magnetochemische Untersuchungen an Komplexcarbiden. *Monatsh Chem* **97**, 1428-1436 (1966).
23. Lapauw T., Tunca B., Potashnikov D., Pesach A., Ozeri O., Vleugels J., *et al.* The double solid solution $(Zr, Nb)_2(Al, Sn)C$ MAX phase: a steric stability approach. *Sci Rep* **8**, 12801 (2018).
24. Halim J., Palisaitis J., Lu J., Thörnberg J., Moon E. J., Precner M., *et al.* Synthesis of Two-Dimensional $Nb_{1.33}C$ (MXene) with Randomly Distributed Vacancies by Etching of the Quaternary Solid Solution $(Nb_{2/3}Sc_{1/3})_2AlC$ MAX Phase. *ACS Applied Nano Materials* **1**, 2455-2460 (2018).
25. Pan R., Zhu J., Liu Y. Synthesis, microstructure and properties of $(Ti_{1-x},Mo_x)_2AlC$ phases. *Materials Science and Technology* **34**, 1064-1069 (2018).
26. Hamm C. M., Duerrschnabel M., Molina L., Salikhov R., Spoddig D., Farle M., *et al.* Structural, magnetic and electrical transport properties of non-conventionally prepared MAX phases V_2AlC and $(V/Mn)_2AlC$. *Materials Chemistry Frontiers* **2**, 483-490 (2017).
27. Lin S., Tong P., Wang B. S., Huang Y. N., Lu W. J., Shao D. F., *et al.* Magnetic and electrical/thermal transport properties of Mn-doped $M_{n+1}AX_n$ phase compounds $Cr_{2-x}Mn_xGaC$ ($0 \leq x \leq 1$). *J Appl Phys* **113**, 053502 (2013).
28. Petruhins A., Ingason A. S., Lu J., Magnus F., Olafsson S., Rosen J. Synthesis and characterization of magnetic $(Cr_{0.5}Mn_{0.5})_2GaC$ thin films. *J Mater Sci* **50**, 4495-4502 (2015).
29. Lai C.-C., Tao Q., Fashandi H., Wiedwald U., Salikhov R., Farle M., *et al.* Magnetic properties and structural characterization of layered $(Cr_{0.5}Mn_{0.5})_2AuC$ synthesized by thermally induced substitutional reaction in $(Cr_{0.5}Mn_{0.5})_2GaC$. *APL Mater* **6**, 026104 (2018).
30. Meshkian R., Ingason A. S., Arnalds U. B., Magnus F., Lu J., Rosen J. A magnetic atomic laminate from thin film synthesis: $(Mo_{0.5}Mn_{0.5})_2GaC$. *APL Mater* **3**, 076102 (2015).
31. Gupta S., Hoffman E. N., Barsoum M. W. Synthesis and oxidation of Ti_2InC, Zr_2InC, $(Ti_{0.5},Zr_{0.5})_2InC$ and $(Ti_{0.5},Hf_{0.5})_2InC$ in air. *J Alloys Compd* **426**, 168-175 (2006).
32. Manoun B., Leaffer O. D., Gupta S., Hoffman E. N., Saxena S. K., Spanier J. E., *et al.* On the compression behavior of Ti_2InC, $(Ti_{0.5},Zr_{0.5})2InC$, and M_2SnC (M = Ti, Nb, Hf) to quasi-hydrostatic pressures up to 50 GPa. *Solid State Commun* **149**, 1978-1983 (2009).
33. Barsoum M. W., Golczewski J., Seifert H. J., Aldinger F. Fabrication and electrical and thermal properties of Ti_2InC, Hf_2InC and $(Ti,Hf)_2InC$. *J Alloys Compd* **340**, 173-179 (2002).

34. Kerdsongpanya S., Buchholt K., Tengstrand O., Lu J., Jensen J., Hultman L., *et al.* Phase-stabilization and substrate effects on nucleation and growth of $(Ti,V)_{n+1}GeC_n$ thin films. *J Appl Phys* **110**, 053516 (2011).
35. Lin S., Huang Y., Zu L., Kan X., Lin J., Song W., *et al.* Alloying effects on structural, magnetic, and electrical/thermal transport properties in MAX-phase $Cr_{2-x}M_xGeC$ (M =Ti, V, Mn, Fe, and Mo). *J Alloys Compd* **680**, 452-461 (2016).
36. Phatak N. A., Saxena S. K., Fei Y., Hu J. Synthesis of a new MAX compound $(Cr_{0.5}V_{0.5})_2GeC$ and its compressive behavior up to 49 GPa. *J Alloys Compd* **475**, 629-634 (2009).
37. Scabarozi T. H., Benjamin S., Adamson B., Applegate J., Roche J., Pfeiffer E., *et al.* Combinatorial Investigation of the Stoichiometry, Electronic Transport and Elastic Properties of $(Cr_{1-x}V_x)_2GeC$ Thin Films. *Scripta Mater* **66**, 85-88 (2011).
38. Ingason A. S., Mockute A., Dahlqvist M., Magnus F., Olafsson S., Arnalds U. B., *et al.* Magnetic self-organized atomic laminate from first principles and thin film synthesis. *Phys Rev Lett* **110**, 195502 (2013).
39. Liu Z., Waki T., Tabata Y., Nakamura H. Mn-doping-induced itinerant-electron ferromagnetism in Cr_2GeC. *Phys Rev B* **89**, 054435 (2014).
40. Rivin O., Caspi E. N., Pesach A., Shaked H., Hoser A., Georgii R., *et al.* Evidence for ferromagnetic ordering in the MAX phase $(Cr_{0.96}Mn_{0.04})_2GeC$. *Mater Res Lett* **5**, 465-471 (2017).
41. Tao Q., Dahlqvist M., Lu J., Kota S., Meshkian R., Halim J., *et al.* Two-dimensional $Mo_{1.33}C$ MXene with divacancy ordering prepared from parent 3D laminate with in-plane chemical ordering. *Nat Commun* **8**, 14949 (2017).
42. Dahlqvist M., Lu J., Meshkian R., Tao Q., Hultman L., Rosen J. Prediction and synthesis of a family of atomic laminate phases with Kagomé-like and in-plane chemical ordering. *Sci Adv* **3**, e1700642 (2017).
43. Lu J., Thore A., Meshkian R., Tao Q., Hultman L., Rosen J. Theoretical and experimental exploration of a novel in-plane chemically-ordered $(Cr_{2/3}M_{1/3})_2AlC$ i-MAX phase with *M*=Sc and Y. *Cryst Growth Des* **17**, 5704–5711 (2017).
44. Meshkian R., Dahlqvist M., Lu J., Wickman B., Halim J., Thörnberg J., *et al.* W-based atomic laminates and their 2D derivative $W_{1.33}C$ MXene with vacancy ordering. *Adv Mater* **30**, 1706409 (2018).
45. Chen L., Dahlqvist M., Lapauw T., Tunca B., Wang F., Lu J., *et al.* Theoretical Prediction and Synthesis of $(Cr_{2/3}Zr_{1/3})_2AlC$ *i*-MAX Phase. *Inorg Chem* **57**, 6237-6244 (2018).
46. Thörnberg J., Halim J., Lu J., Meshkian R., Palisaitis J., Hultman L., *et al.* Synthesis of $(V_{2/3}Sc_{1/3})_2AlC$ *i*-MAX phase and $V_{2-x}C$ MXene scrolls. *Nanoscale* **11**, 14720-14726 (2019).
47. Tao Q., Lu J., Dahlqvist M., Mockute A., Calder S., Petruhins A., *et al.* Atomically Layered and Ordered Rare-Earth i-MAX Phases: A New Class of Magnetic Quaternary Compounds. *Chem Mater* **31**, 2476-2485 (2019).
48. Dahlqvist M., Petruhins A., Lu J., Hultman L., Rosen J. Origin of Chemically Ordered Atomic Laminates (i-MAX): Expanding the Elemental Space by a Theoretical/Experimental Approach. *ACS Nano* **12**, 7761-7770 (2018).
49. Petruhins A., Dahlqvist M., Lu J., Hultman L., Rosen J. Theoretical prediction and experimental verification of the chemically-ordered atomic-laminate *i*-MAX phases $(Cr_{2/3}Sc_{1/3})_2GaC$ and $(Mn_{2/3}Sc_{1/3})_2GaC$. *Cryst Growth Des* **20**, 55-61 (2020).

50. Petruhins A., Lu J., Hultman L., Rosen J. Synthesis of atomically layered and chemically ordered rare-earth (RE) *i*-MAX phases; $(Mo_{2/3}RE_{1/3})_2GaC$ with RE = Gd, Tb, Dy, Ho, Er, Tm, Yb, and Lu. *Mater Res Lett* **7**, 446-452 (2019).
51. Greenwood N. N., Earnshaw A. *Chemistry of the Elements* (Butterworth-Heinemann, 1997).
52. Huheey J. E., Keiter E. A., Keiter R. L. *Inorganic Chemistry : Principles of Structure and Reactivity* (HarperCollins, New York, USA, 1993).